NASA CR-72603

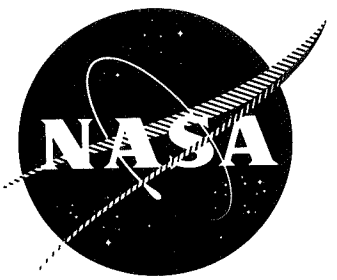

COMPATIBILITY TESTING OF CANDIDATE PROTECTIVE BARRIER COATINGS AND PERFORMANCE TESTING OF FILTER VENT MATERIALS

by

W. R. Seetoo and J. W. McGrew

prepared for

NATIONAL AERONAUTICS AND SPACE ADMINISTRATION

Contract NAS 3-11839

ISOTOPES
NUCLEAR SYSTEMS DIVISION
A TELEDYNE COMPANY

Requests for copies of this report should be referred to

National Aeronautics and Space Administration
Scientific and Technical Information Facility
P. O. Box 33
College Park, Md. 20740

NASA CR-72603

FINAL REPORT

COMPATIBILITY TESTING OF CANDIDATE PROTECTIVE BARRIER COATINGS AND PERFORMANCE TESTING OF FILTER VENT MATERIALS

by

W. R. Seetoo and J. W. McGrew

ISOTOPES
Nuclear Systems Division
110 West Timonium Road
Timonium, Maryland 21093

prepared for

NATIONAL AERONAUTICS AND SPACE ADMINISTRATION

June 16, 1969

CONTRACT NAS 3-11839

NASA Lewis Research Center
Cleveland, Ohio
Hubert P. Smreker, Project Manager
Nuclear Systems Division

TABLE OF CONTENTS

LIST OF FIGURES

LIST OF TABLES

ABSTRACT

Tantalum specimens were coated with Al_2O_3 or ZrO_2. The coated specimens were subjected to bend tests, corrosion in lithium pentaborate solution, exposed to wet hydrogen at high temperature and exposed to simulated molten reactor fuels. The Al_2O_3 coating spalled but the ZrO_2 coating was intact after the bend test. Both coatings were unaffected by the lithium pentaborate solution. Both coatings were impervious to molten simulated fuel.

ZrO_2 and Al_2O_3 were evaluated as filter vent materials for hydrogen, helium, xenon and a mixture of these gases at various temperatures and pressures. Room temperature helium flow rates varied from 1.11 std. cc/sec to 6.7×10^{-8} std. cc/sec, depending on filter material, filter geometry and gas backpressure. The elevated temperature flow rates for helium, hydrogen and xenon were anomalous due to numerous variables such as material expansion differences, gas purity, absence of sufficient data points, thermal cycling and vent blockage. Problem areas are pinpointed and discussed.

SUMMARY

Two flame-sprayed ceramic coatings, Al_2O_3 and ZrO_2, were evaluated as protective barrier coatings for a tantalum catch basin in a reactor vessel. The coatings were evaluated for adherence after coating, after exposure to simulated molten fuel, and after exposure to a 3 weight percent lithium pentaborate solution. The Al_2O_3 coating spalled on both sides in a bend test and the ZrO_2 coating spalled on the interior but not on the exterior of the bend.

Coated coupons were autoclave tested in a 3 weight percent lithium pentaborate solution. The rods were completely coated while the coupons were coated on the faces only. Both coatings were intact after the tests with no evidence of spalling, cracking, blistering or peeling.

Fused reactor fuels or claddings or mixtures thereof were dropped into cold tantalum cups coated with either Al_2O_3 or ZrO_2. The three test formulations were Type 304 stainless steel, an equal weight mixture of depleted UO_2-Mo, and an equal weight mixture of Type 304 stainless steel-Mo-UO_2. There was no apparent reaction between any of the three simulated fuels and the two coatings. Some slight cracking of both coatings occurred with the latter two fuel mixtures. Both coatings are satisfactory in preventing molten fuel from contacting the tantalum catch basin and reacting with it.

Two tantalum cups, one of each coated with Al_2O_3 and ZrO_2 and each containing one of the simulated fuels, stainless steel-molybdenum-UO_2, were tested in moist hydrogen at high temperature. Unfortunately, the cups had been coated only on their interior surfaces. While this was sufficient for the other tests, on this test the exterior surface was inadvertently left unprotected from the hydrogen atmosphere. As a result, the tantalum substrate of both cups disintegrated, leaving the coating as a thin shell. When examined metallographically, it was found that there was no reaction between the ZrO_2 and the fuel, but the fuel reacted with the Al_2O_3 and migrated through the coating.

Six filter vents were fabricated and tested for selectivity in venting helium, hydrogen, xenon and a mixture of these gases at various temperatures and pressures. Two materials were investigated, ZrO_2 and Al_2O_3, in various geometries. The leak rates were found to be a function of the filter element density, diameter and length. The leak rate also varied with gas temperature, pressure and molecular or atomic size. The filters were flow tested with helium at room temperature at various gas backpressures, then with helium, hydrogen, xenon individually and a 50:50:1 mixture of the preceding gases at several different filter temperatures and 100 PSIA (6.89×10^5 N/m) gas backpressure. Room temperature helium flow rates ranged from 1.11 std. cc/sec to 6.7×10^{-8} std. cc/sec depending on filter material,

filter geometry, and gas backpressure. The elevated temperature flow rates for helium, hydrogen and xenon were anomalous due to numerous variables such as material expansion differences, gas purity, insufficient data points, thermal cycling and vent blockage. Problem areas are pinpointed and discussed.

INTRODUCTION

The purpose of this program was to evaluate candidate protective barrier coatings and selective vent materials for use in the Multi-Purpose Nuclear Aircraft (MNA). In the event of a core meltdown it is desirous to retain the molten material within the reactor vessel. Since the molten fuel might react with the tantalum catch basin material and permit eventual release of radioactive materials, two barriers which could potentially prevent this occurrence were evaluated. The barrier coatings were ZrO_2 and Al_2O_3. An attempt was made to evaluate UO_2 also as a coating material, but the coating process was unsuccessful. To be effective, the coatings should be adherent to the tantalum and should not react with molten reactor fuel. Samples of each coating were subjected to bend tests and exposed to simulated molten fuel. Metallographic examination of typical test areas were made and each coating was evaluated for adherence and compatibility.

In addition to controlling the release of radioactive solids in the event of a core meltdown, it is also desirous to retain radioactive gases within the reactor vessel. However, the non-radioactive gases could be vented to prevent excessive gas pressure within the reactor containment vessel. This program evaluated two vent materials, ZrO_2 and Al_2O_3, for selectivity in venting H_2, He and Xe gas at room temperature and at elevated temperatures.

The technology upon which the filter vent work was based resulted from an earlier successful vent development program. In that program a concept for venting a single gas, helium, was finalized and perfected. All testing was done at room temperature with a maximum backpressure of 20 psia. The objective of the program was to provide a maximum helium vent rate but retain a radioactive species of very small particle size. Relatively low density zirconia filter elements bonded into Haynes 25 housings met the criteria. The flow rates ranged from 10^{-1} to 10^{-3} cc/sec (12.3 cc/sec-cm^2 to 0.12 cc/sec-cm^2) with an L/D of 2.25. Relatively low density alumina elements of the same L/D ratio had flow rates five to six magnitudes lower.

It was the intent of this current program to use precisely the same design and fabrication concept and vary appropriately the filter element geometry and density only. Further, it was intended only to measure and report the flow rates of the individual and mixed gases and determine the applicability of this filter concept at its current state of development to this particular gas venting problem.

The effects of several parameters were postulated. These included the effects of L/D ratio and density of the filter element, backpressure of the test gas, test temperature, molecular or atomic size, and thermal expansion.

The effort was divided among four tasks:

TASK 1 - Fabrication and Coating of Containment Vessels and Specimens

TASK 2 - Fabrication and Installation of Filter Vent Materials

TASK 3 - Compatibility Testing of Protective Barrier Coatings

TASK 4 - Performance Testing of Filter Vent Materials

Each of these tasks will be discussed individually in detail in the next section.

EXPERIMENTAL PROCEDURE

A. TASK 1 - Fabrication and Coating of Containment Vessels and Specimens

The scope of this task included fabricating and coating tantalum cups, coupons and rods for compatibility testing and coating evaluation.

Thirty-mil (7.62×10^{-4}m) thick tantalum sheet was procured and quality inspected to assure a uniform thickness to $\pm$ 0.002 inch ($\pm 5.08 \times 10^{-5}$m). After inspection, the tantalum sheet was sheared and discs punched to permit fabrication of nine cups 3 inches (7.62×10^{-2}m) outside diameter by 1/2 inch (1.27×10^{-2}m) deep, three cups 1 inch (2.54×10^{-2}m) outside diameter by 1 inch (2.54×10^{-2}m) deep, and twelve coupons 1 inch (2.54×10^{-2}m) wide by 4 inches (1.016×10^{-1}m) long. A 1/2 inch (1.27×10^{-2}m) diameter tantalum rod was cut into three pieces 2-1/4 inches (5.72×10^{-2}m) long and the sharp edges were rounded off to a 1/32 inch (8.13×10^{-4}m) radius.

The cups were welded in argon by the tungsten inert gas (TIG) process with 100% penetration at the seams. The seams were machined on the interior of the cups to present a flush, smooth surface on the wall and a 1/32 inch (8.13×10^{-4}m) radius at the bottom. After the cups were fabricated, cups, coupons and rods were grit blasted with 120 mesh steel and chemically cleaned to remove all iron remnants. These specimens are shown in Fig. 1 After cleaning, all samples were stored at room temperature in plastic bags in a vacuum oven to await coating.

The difference in thermal expansion between the tantalum substrate and the ceramic coating made it necessary to plasma spray a tantalum transition coat prior to coating with the Al_2O_3, ZrO_2 or UO_2. Spraying was done with a Plasma Arc torch at the following settings:

Tip	#57 x 34; 0.219 inch diameter (5.56×10^{-3}m)
Gas	100 CFH argon (7.863×10^{-1}m^3/s); 4 CFH hydrogen (3.145×10^{-2}m^3/s)
Voltage	Arc 500 + 15; 44 $\pm$ 5DC
Powder Flow	7 CFH argon (5.504×10^{-2}m^3/s)

The tantalum powder used was Metco #62, -200 +325 mesh, and was sprayed to a thickness of 1 mil (2.54×10^{-5}m) on a test coupon. This coupon was bent 180° to determine coating adherence. The coating was tightly adherent on the exterior of the bend but spalled on the interior, probably due to mechanical damage by the mandrel. Samples fabricated for a previous program were heat treated prior to bend testing, therefore it was decided to heat treat all samples prior to any other tests.

A special jig was made for rotating the cups while they were being coated with tantalum and the ceramic coatings. A special hood was set up for spraying the depleted UO_2 material which still has some residual radioactivity. All other spraying was done in the metal and ceramic spray facility.

No problems were encountered in spraying the tantalum onto the cups, coupons or rods. The Al_2O_3 and ZrO_2 coatings were applied with a Metco Flame Spray Gun (Mogul R-3). These specimens are shown in Fig. 2. The coatings were applied in several passes until a thickness of 5 mils (1.27×10^{-4}m) was obtained. Spray data for each coating are as follows:

Al_2O_3 Norton aluminum oxide Rokide A, BLH-4
1/4 inch diameter x 18 inches (6.35×10^{-3}m x 4.57×10^{-1}m)
Gas Data: Acetylene 21 PSI (1.45×10^5 N/m^2) 45 on flowmeter
Oxygen 42 PSI (2.89×10^5 N/m^2) 35 on flowmeter
Air 95 PSI (6.55×10^5 N/m^2)
Rod Speed: 3-20 Setting

ZrO_2 Norton zirconium oxide zirconite
1/4 inch diameter x 19-1/2 inches (6.35×10^{-3}m x 4.95×10^{-1}m)
Gas Data: Same as for Al_2O_3
Rod Speed: Same as for Al_2O_3

The UO_2 powder was sprayed with a Metco Thermal Spray Gun, Type 2P, in the specially built hood. The powder was a depleted ceramic grade -325 mesh from Nuclear Fuel Services. It did not flow readily and much difficulty in maintaining a spray was encountered. The powder was cold compacted, crushed and sieved to obtain a -100 +120 mesh fraction which flowed readily. This powder was sprayed at the following settings:

Oxygen 14 PSI (9.65×10^4 N/m^2)
Acetylene 12 PSI (8.27×10^4 N/m^2) Flow Rate 30 Setting
Powder Flow 4 - Vibrator on

The powder appeared molten, but, when it struck the tantalum, it bounced off instead of adhering. Many passes were required to obtain any build-up of UO_2 on the tantalum. During the coating process, the tantalum became discolored from oxidation as a result of the many passes required to effect any thickness. Attempts to air cool from the back did not solve the problem. Since spraying of UO_2 was not a developed "state of the art", permission to delete this coating from the statement of work was requested of NASA and further work in this area was discontinued.

The remaining specimens were heat treated in vacuum to improve the strength of the ceramic to tantalum bond. The heat treatment consisted of heating the specimens while under vacuum to 1400°C (1673°K) and slowly cooling. The samples were heated at a pressure of 1.4×10^{-4} torr (1.866

x 10^{-2} N/m^2) or lower to 1400°C (1673°K) in 1 hour (3600 sec) and allowed to furnace cool overnight. All coatings were bright and clean with no evidence of cracks, blisters or spalling. A metallographic section of the Al_2O_3 and ZrO_2 coatings is shown in Figs. 3 and 4.

B. TASK 2 - Fabrication and Installation of Filter Vent Elements

Two materials were investigated as filter elements. These materials were Al_2O_3 and ZrO_2 which are known commercially as Lucalox and Rokide Z or stabilized vitreous zirconium oxide respectively. Four filters, two alumina and two zirconia, have an L/D ratio of 2.25, and two filters, one each of alumina and zirconia have an L/D ratio of $\sim$0.57.

The filter vents were ground into circular rods with nominal dimensions of 0.040 inch diameter (1.016 x 10^{-3}m) or 0.078 inch diameter (1.98 x 10^{-3}m). After grinding, the elements were platinum plated on the outside diameter to increase the diameter by 0.010 inch (2.54 x 10^{-4}m). The platinum plating procedure used is given below:

1. Clean preground vent in denatured alcohol.
2. Paint (with a brush) vent with duPont Liquid Bright Platinum #7447.
3. Fire vent for 30 minutes (1800 sec) at 610°C (883°K), remove from furnace and air cool.
4. Wipe vent with alcohol.
5. Repeat Steps 2, 3 and 4 until surface is uniformly coated.
6. Wipe vent with alcohol.
7. Prepare a plating solution composed of 1 part distilled water to 2 parts of Englehard #209 platinum plating solution.

    a. Plating conditions are: Platinum anode, solution temperature 88-93°C (361 to 366°K) pH 10, continuous agitation, 40-60 milliamps DC current per vent.
    b. Every 15 minutes (900 sec) reverse DC current for 30 seconds (makes plate less porous).

    c. Every 30 minutes (1800 sec) rotate sample 120° in holder.

8. At end of an 8 hour (2.88 x 10^4 sec) day measure plating thickness (it usually takes 2-3 eight hour days to get a 10 mil (2.54 x 10^{-4}m) thickness on the O.D.).

After plating, the vents were reground to an O.D. of 0.0402 inch 1.021 x 10^{-3}m) or 0.0782 inch (1.986 x 10^{-3}m) and faced off to a length of 0.090 inch (2.286 x 10^{-3}m) or 0.045 inch (1.143 x 10^{-3}m). The reground vents were then inserted into a Haynes 25 housing, using a special insertion tool and then diffusion bonded for 76 hours (2.73 x 10^5 sec) at 760°C (1033°K) at a pressure of 10^{-5} torr (1.333 x 10^{-3} N/m^2) or lower. Table I shows the fabricated filter materials, geometries and densities, while Fig. 5 shows the processing steps involved in preparing an assembly.

After the diffusion treatment, the Haynes 25 housing with the filter vent was TIG welded into a 1/2 inch (1.27×10^{-2}m) diameter Haynes 25 tube to permit room and elevated temperature testing in the gas flow test console. Figures 6 and 7 show the method of welding the Haynes 25 housing into the Haynes 25 tubes. The tube on the right is tapered to permit a good fit-up with the housing. The housing is then welded into the tube. A larger Haynes 25 tube is slipped over the machined ends of the two tubes and welded at the circumference at both tubes to complete the joint. This method of welding is necessary to prevent overheating of the filter vent. The ends of the Haynes 25 tubes are connected into the flow console with Swagelok connectors.

C. TASK 3 - Compatibility Testing of Protective Coatings

1. Bend Tests

A bend test form was fabricated to permit 180° bends in the coated coupons. The form consisted of two anvils which support the coupon. A third anvil with a 1/2 inch (1.27×10^{-2}m) diameter rod went between the other two anvils and bent the coupon 180° over the 1/2 inch (1.27×10^{-2}m) diameter rod. Tests with samples indicated that the form put a severe stress on the interior of the bend.

One Al_2O_3 coated coupon and one ZrO_2 coated coupon were bent to evaluate coating adherence. Both cracked and spalled on the interior of the bend, but the Al_2O_3 coated coupon also cracked and spalled about 1/8 inch (3.175×10^{-3}m) in from the edges on the exterior of the bend. The ZrO_2 coating did not crack but spalled about 1/32 inch (8.13×10^{-4}m) in from the edges of the exterior bend. The bent coupons are shown in Figs. 8 and 9. This test indicated that the ZrO_2 coating is somewhat more formable than the Al_2O_3.

2. Meltdown Tests

Simulated fuel pellets were cold pressed and sintered for use in meltdown tests in the coated cups. The simulated pellets consisted of undiluted Type 304 stainless steel, 50 weight percent depleted UO_2 - 50 weight percent molybdenum, and 33-1/3 weight percent Type 304 stainless steel - 33-1/3 weight percent molybdenum - 33-1/3 weight percent depleted UO_2. Pertinent data for the powders used are as follows:

Stainless Steel	Vanadium Alloys Steel Co. Type 304 - 230 mesh - PVS 7057
Molybdenum	Sylvania Electric Co. Lot #MOT 2682-C
UO_2	Nuclear Fuel Services Depleted ceramic grade Purchase Order #4E-0134

Three pellets, 1-1/2 inch (3.81×10^{-2}m) in diameter, were fabricated for each of three powder mixtures, and three additional pellets, 0.75 inch (1.91×10^{-2}m) in diameter, containing the stainless steel-molybdenum-UO_2, were fabricated for wet hydrogen test.

The pellets were fabricated by hand mixing the as-received powders with an acetone solution containing 1 weight percent stearic acid. The moist powder was dried under a heat lamp, then cold compacted in an appropriately sized die at 5 tons per square inch (TSI) (6.895×10^{7} N/m^2) pressure. After cold compacting, the pellets were sintered in a hydrogen atmosphere for 1 hour (3600s). The pellets were stoked into the hot zone very slowly to permit the stearic acid die lubricant to burn off without damage to the pellet. The pellets were sintered at the temperatures listed below:

Pellets containing Type 304 stainless steel	1100°C (1373°K)
Pellets containing UO_2-Molybdenum	1400°C (1673°K)

All pellets were intact after sintering and could be handled readily without danger of breaking, as illustrated in Fig. 10.

Two triangular holders were fabricated from tungsten rod to hold the fuel pellet so it would fall into the coated cup in the molten condition. The smaller triangular holder for the 0.75 inch (1.91×10^{-2}m) diameter fuel pellet was fabricated from 3/32 inch (2.36×10^{-3}m) diameter rod while the holder for the 1.5 inch (3.81×10^{-2}m) diameter pellets was fabricated from 1/4 inch (6.35×10^{-3}m) rod. These holders spanned the edge of the cup and were grounded to the arc melter hearth plate with a heavy copper strap. The pellet was placed upon the holder and an arc struck to melt out the center portion of the pellet. In order to drop the molten fuel into the cup, power to the arc was increased to melt through the bottom of the "skull" and allow the molten fuel to pour into the cup.

Trial melts with test stainless steel pellets were made to determine the meltdown parameters and arc melting procedures. The following procedure was established for arc melting the simulated fuel:

a. Evacuate chamber to 25 microns (3.333 N/m^2)
b. Backfill with argon to 760 mm Hg (1.013×10^{5} N/m^2)
c. Repeat a. and b. two more times.
d. On third backfill, backfill with argon to 456 mm Hg (6.08×10^{4} N/m^2), then with helium to 507 mm Hg (6.76×10^{4} N/m^2).
e. Strike arc on titanium getter button and melt, then quickly transfer arc to stainless steel pellet. Melt interior of pellet at low amperage, then increase amperage suddenly when ready to melt through bottom.

Attempts to melt in pure helium were unsuccessful because an arc could not be struck with a high concentration of helium. The above meltdown procedure had to be modified for the pellets containing UO_2. When these

pellets were melted, some constitutent (most likely UO_2) volatilized and coated the interior surfaces of the chamber (including the coated cup) and the sight glass making it impossible to see when the pellet became completely molten. The meltdown procedure was modified to the following:

a. Place pellet on arc melter hearth plate and evacuate to 25 microns (3.333 N/m^2) and backfill with argon. Repeat three times. Backfill the last time to 456 mm Hg (6.08×10^4 N/m^2) with argon, then to 507 mm Hg (6.76×10^4 N/m^2) with helium. Do initial melt until sight glass fogs up.

b. Allow pellet to cool, evacuate system, backfill with argon, remove sight glass and clean.

c. Repeat evacuation and melting as detailed in Step a.

Each pellet containing UO_2 required about 4 to 6 melt cycles before the pellet was sufficiently solid enough to greatly reduce the volatilization and fogging problem. Then the pellet was placed on the tungsten holder over the cup and melted a final time to drop the molten material into the coated cup.

The brown soot (from the volatilization of the UO_2) covered the interior of the coated cups. The resulting very thin film of UO_2 probably does not have an effect on the compatibility test.

The melting parameters for the various pellets are given below:

a.	Stainless Steel	16 volts and 150 amperes
b.	Molybdenum-UO_2	40-42 volts and 350-400 amperes
c.	Molybdenum-SS-UO_2	40-42 volts and 350-400 amperes

After meltdown, the cups were examined visually (see Fig.11) and metallographically (see Figs. 12 to 17) for coating cracking, reaction, spalling, etc. The results of this examination were as follows:

a. Stainless steel on Al_2O_3 coated cup

Visual: The stainless steel did not stick to the cup and there was no evidence of cracking, blistering or spalling.

Metallographic: No cracks were evident in the coating. The coating was still adherent to the tantalum. There was no reaction between the molten stainless steel and the coating.

b. Stainless steel on ZrO_2 coating

Visual: Same as for the Al_2O_3 coating.

Metallographic: Same as for the Al_2O_3 coating. There was more porosity evident in this coating than in the Al_2O_3 coating.

c. Mo-UO_2 on Al_2O_3 coated cup

Visual: The molten material adhered to the coating and appeared to have reacted. When pried, the coating appeared to adhere to the molten fuel, exposing the tantalum substrate.

Metallographic: Coating had cracked in several places. In the area where the coating adhered to the fuel, the separation occurred between the tantalum powder coating and the wrought tantalum. There was no reaction between the fuel and the coating. The adherence appeared to be strictly mechanical.

d. Mo-UO_2 on ZrO_2 coated cup

Visual: The molten material adhered to the coating but when pried did not pull the coating away from the tantalum.

Metallographic: Some cracks were present and more porosity evident than in the Al_2O_3 coating. No reaction occurred between the fuel and coating. Coating was still adherent to the tantalum.

e. SS-Mo-UO_2 on Al_2O_3 coated cup

Visual: The molten material adhered to the coating and when pried a portion of the coating pulled away while another part adhered.

Metallographic: In the area where the coating adhered to the fuel, a slight reaction was noted. However, the fuel did not penetrate the coating. There was some porosity present in the coating. In the adherent portion of the coating there were no cracks and the coating was still well bonded.

f. SS-Mo-UO_2 on ZrO_2 coated cup

Visual: The molten material adhered to the coating and, when pried, most of the coating adhered to the molten material exposing the tantalum.

Metallographic: The coating that adhered to the fuel was intact with no cracks. Some porosity was present in the coating. There was no evidence of reaction between coating and fuel. The bond between the fuel and coating was probably mechanical.

These tests show that either Al_2O_3 or ZrO_2 coatings are suitable for protecting tantalum from a molten fuel. The ZrO_2 coatings are more porous than the Al_2O_3 coatings, yet they are more adherent. Possibly the porosity absorbs some of the stresses.

3. Wet Hydrogen Test

Samples of the stainless steel-molybdenum-UO_2 were melted into an Al_2O_3 and ZrO_2 coated cup for wet hydrogen tests. The cups were 1 inch (2.54×10^{-2}m) in diameter by 1 inch (2.54×10^{-2}m) high. The simulated fuel pellets weighed 90 grams and were 0.75 inch (1.91×10^{-2}m) in diameter. A bubbler was fabricated to permit introduction of moisture into the incoming hydrogen. A dew point apparatus and bypass were installed in the same line so the hydrogen could be monitored during the test. The wet hydrogen was introduced into the furnace and stabilized at $0^{\circ}C$ ($273^{\circ}K$) dew point prior to insertion of the samples. The samples were stoked slowly into the hot zone to minimize thermal shock to the coatings. After 4 hours (1.44×10^{4}s) at $1700^{\circ}C$ ($1973^{\circ}K$), as measured with an optical pyrometer, the samples were slowly stoked into the cold zone and the bubbler was shut off.

Upon examination, the tantalum had disintegrated leaving the fuel laying on a thin skin of Al_2O_3 or ZrO_2. The tantalum that remained was extremely brittle and complete recrystallized. Since the cups were coated only on the interior, the coating did not protect the tantalum substrate from the moisture in the hydrogen. Tantalum must be treated in vacuum or completely coated when operated at elevated temperatures in order to retain its strength properties.

The simulated fuel that had adhered to the coatings was examined metallographically. The fuel in contact with the ZrO_2 coating had not reacted even though it stuck to the coating. The coating was quite porous and there was no tantalum remaining beneath the ZrO_2 coating. The fuel in contact with the Al_2O_3 had reacted and had migrated across the coating. The coating was cracked in several places and in areas where some tantalum was present, the coating had pulled away. This test showed that a ZrO_2 coating is more suitable than an Al_2O_3 coating in preventing molten fuel from contacting tantalum under the test conditions used.

4. Lithium Pentaborate Test

Several coupons and rods were tested for 500 and 1000 hours (1.8×10^6 and 3.6×10^6 sec) at 150°C (423°K) in a 3 weight percent lithium pentaborate solution. The tests were run in two separate autoclaves, one being operated for 500 hours (1.8×10^6 sec) and the other 1000 hours (3.6×10^6 sec). The autoclaves were rinsed thoroughly with deionized water, then filled with 2 liters of 3 weight percent lithium pentaborate solution. Next the coupons and rods were placed into the solution but standing on one end and leaning against the autoclave wall. All samples were completely immersed in the solution. The autoclaves were closed up and evacuated to 0.5 inches of mercury (1.013×10^{-1} N/m^2) for five minutes to outgas the water, then backfilled with argon to atmospheric pressure. Power was applied and the temperature raised until the steam pressure was 69 ± 5 psi ($4.757 \times 10^5 \pm 3.447 \times 10^4$ N/m^2). This is equivalent to a temperature of 150 ± 3°C (423 ± 3°K).

After 500 hours (1.8×10^6 sec), one autoclave was shut down and the samples were examined. There was no evidence of cracking, blistering, peeling or spalling of either the Al_2O_3 or ZrO_2 coatings. After 1000 hours (3.6×10^6 sec), the other autoclave was shut down. These samples also were intact with no cracks, blisters, peeling or spalling, as shown in Fig. 18. The tantalum substrate was not attacked by the pentaborate solution after the 500 and 1000 hour (1.8×10^6 sec, 3.6×10^6 sec) test.

This test showed that either a ZrO_2 or Al_2O_3 coating adheres to tantalum satisfactorily and that tantalum is unaffected by lithium pentaborate under the above test conditions.

D. TASK 4 - Performance Testing of Filter Vent Materials

The filter vents fabricated in Task 2 were to be tested at room and elevated temperatures with three different gases at various gas pressures. A test console was assembled to permit testing of the filters. Fig. 19 is a sketch of the console layout.

Each filter was tested with helium at room temperature with gas pressures ranging from 20 to 200 psia (1.38×10^5 N/m^2 to 1.38×10^6 N/m^2) in 20 psi (1.38×10^5 N/m^2) increments. Then the filters were heated to 500°C (773°K) and tested with helium, hydrogen, xenon individually and with a 50:50:1 mixture by pressure of helium, hydrogen, xenon at a total pressure of 100 psia (6.89×10^5 N/m^2). The elevated temperature test was repeated with the same gases at 850°C and 1050°C (1123 and 1323°K).

The equipment used in determining the permeability or gas flow rates consisted of a Veeco Residual Gas Analyzer Model GA-4 and a Veeco VS-400 Pumping Station. A Veeco MS-9 Leak Detector was used to check the system for leaks after installation of the filter. A Hevi Duty 1500 Watt Split Tube Furnace was used to heat the filters to the desired temperature. Temperatures were maintained to ± 5°C (± 5°K) with a Variac power control. A Chromel-alumel thermocouple was spot tacked to the Haynes 25 tubing at the filter location and millivolt output

was read from a Rubicon potentiometer. Source pressures (PSIA) were read on calibrated 6 inch (1.5×10^{-1}m) Heise gauges to the nearest half pound pressure (3.45×10^3 N/^{2}).

1. Test Procedure

The procedure established for testing the filters was as follows:

a. Install filter vent into test system with Swagelok connectors.

b. Evacuate the entire system with the pumping station and the residual gas analyser (RGA) roughing pump. Leak test the system.

c. Isolate the downstream side of the system from the vacuum pump and continue to pump on the downstream side with the high vacuum system of the RGA.

d. Calibrate the response of the RGA to the test gas by opening the standard leak. Close leak after calibration.

e. Isolate the gas reservoir from the rest of the system and pressurize with test gas to a pressure above the highest test pressure required.

f. Isolate the remainder of the system from the vacuum pump. Bleed test gas to the upstream side of the filter until the first test pressure is obtained. Read flow rate through filter on RGA.

g. Bleed more gas from the gas reservoir to the upstream side of the filter until second test pressure is obtained. Read flow rate on RGA.

h. Repeat Step g. until completion of test.

i. For elevated temperature test, the furnace is turned on after Step b. Test pressure is always 100 psia (6.895×10^5 N/m^2).

j. To change gases, isolate gas inlet, evacuate entire system, hook up new gas and proceed as above.

k. To mix gases, pressurize gas reservoir with desired amount of each gas.

It is necessary to introduce a calibrated leak into the system prior to testing for each gas in order to calculate the leak rate of the gas being tested through the filter. (See Appendix A)

2. Test Results

Six filter elements, three of Al_2O_3 and three of ZrO_2, were tested. Table I lists the filter vent materials, densities, dimensions and housing numbers. The three ZrO_2 vents were numbered 307/9A, 312/4 and 351/333, while the three Al_2O_3 vents were numbered 316/1, 319/13 and 323/20. The densities of two ZrO_2 vents were 5.71 gms/cc while the third was 3.80 gms/cc, and two Al_2O_3 vents were 3.93 gms/cc, while the third was 3.98 gms/cc. It was anticipated that the lower density material would have a greater flow rate than the more dense material; also that the geometry, both cross-sectional area and the L/D ratio, would affect flow rate. Other anticipated results included an increase in flow rate with pressure, an increase in flow rate with temperature, and at any given temperature or pressure a flow rate for the different gases as follows: hydrogen greatest, helium next, and xenon least due to differences in molecular or atomic diameter.

Tables II through XIII tabulate the room and elevated temperature flow rates of the various gases through the six filters tested. Figure 20 is a plot of the room temperature helium flow rates for the same six filters. Elevated temperature flow rates were not plotted because the data were anomalous and, in some instances, inconclusive. The anomalies included instances where the flow rate increased with temperature, then decreased, while in other cases the opposite occurred. Inconclusive tests resulted when data points from a test in progress would be as anticipated, then a flow rate that exceeded the capacity of the RGA detector occurred at the next data point. Since this flow rate could not be given a definite value, a graph could not be plotted. Only three data points were taken at elevated temperature making it impossible to plot flow versus temperature when one or more data points were inconclusive.

All filters were tested at room temperature with a helium back pressure ranging from 20 to 200 psi (1.38×10^5 to 1.38×10^6 N/m^2) prior to being subjected to elevated temperature tests. The order in which the filters were tested was 307, 319, 312, 323, 316 and 351. During the testing of Filter 312, the filament in the Vee tube of the RGA burned out which required replacement. While the RGA was being repaired, it was noted that oil had deposited in the down-stream portion of the vacuum system. This oil was due to "cracking" of the diffusion pump oil which occurred when the water cooling to the pump was interrupted. The RGA was disassembled, cleaned completely, and reinstalled in the test system. Filter 312 was retested with the clean system to see if the flow rate was significantly different because of the "contaminated" RGA. The flow rates were comparable, but the RGA was more sensitive after cleanup.

Figure 20 shows that room temperature flow rates increase fairly linearly with pressure as expected for both Al_2O_3 and ZrO_2. The rate of change with pressure for the 3.80 dense ZrO_2 filter (#351) is about three times that of the 5.71 dense material.

The lower density element, #351, has a flow rate approximately 2.1×10^5 greater on the average than the higher density element, #307. This is probably a reasonable relationship, as is the increased rate of flow for the lower density element with increased backpressure.

In comparing the flow rates of the two higher density (both 5.71 grams/cc) ZrO_2 filters, #307 and #312, it is noted that the larger diameter, shorter length, L/D = 0.57, #312 filter has a much greater flow rate than the smaller diameter #307 Filter of L/D = 2.25. The filter length has a pronounced effect on the flow rate because the area ratio of #312 to #307 is four; therefore, the flow rate, if the length were the same, should be comparable to four. Further, the #312 Filter is one-half the length of #307, so, if the length effect is linear, the flow rate to the shorter element should increase by a factor of two. The two effects combined should be a factor of eight, whereas the measured average difference is about a factor of 250. The most probable explanation is a variability in porosity resulting from a variability in stresses due to thermal effects.

Two Al_2O_3 filters, #319 and #323, were identical in density and dimension. Yet, the average flow rates vary over the range of pressures investigated by about a factor of 2.6. Again, the most probable explanation for this paradox is variation in porosity, although fabrication/assembly variation could contribute to this variability. If these hypotheses are correct, it indicates that, for any given vent material, there is a range of flow rates that can be expected for any given specific geometry at the same density.

The last Al_2O_3 filter, #316, had a greater flow rate than Filters 319 and 323, even though it had a slightly greater density. Apparently the density difference is not the most significant factor in this case, but the change in cross-sectional area and L/D ratio are the controlling factors. Element #316 has an average factor of six greater flow rate than Element #323 and a factor of fifteen greater flow rate than Element #319.

The room temperature helium flow tests showed:

1. Flow rates increase with increasing pressure with both Al_2O_3 and ZrO_2 filters.

2. Low density material has a greater flow rate than high density material in the case of ZrO_2, no direct comparison could be made on the basis of density alone with Al_2O_3.

3. Flow rates are affected by filter geometry with a synergistic effect indicated in the case of ZrO_2. No direct comparison could be made with Al_2O_3.

4. For a given vent material at a given pressure, there is probably a range of flow rates which can be expected (not a specific rate at a given pressure) due to slight variations in raw material fabrication and vent fabrication.

After each filter was flow-tested with helium at room temperature, it was flow-tested at a pressure of 100 psia with helium, hydrogen, xenon and a 50:50:1 mixture of these gases with the filter at 500°C (773°K), 850°C (1123°K), and 1050°C (1323°K).

Filter #307, a high-density ZrO_2 vent, showed a low room temperature flow rate to helium (2.93×10^{-5} std. cc/sec-cm^2) which rapidly increased with increasing temperature (2.80×10^{-1} std. cc/sec-cm^2 at 1050°C), an increase of four magnitudes. A flow rate increase with temperature was expected but the magnitude of the increase was unexpected. All previous work with filter vents had been done with low density ZrO_2 or Al_2O_2 materials. This earlier work was done at low pressures [1-20 psia (6.89×10^3 to 1.38×10^5 N/m^2) helium] and always at room temperature. Therefore, the only reference flow rates available were for low density ZrO_2 or Al_2O_3 at room temperature. These flow rates were for a 0.040 inch diameter by 0.090 inch length (1.02×10^{-3}m x 2.29×10^{-3}m) vent and were on the order of 10^{-1} to 10^{-3} and 10^{-6} to 10^{-8} std. cc/sec at room temperature and 20 psia (1.38×10^5 N/m^2) for the respective vent materials.

When tested with hydrogen, the range of the RGA strip chart was exceeded at 850 and 1050°C (1123 and 1323°K) and efforts to reduce the sensitivity so a reading could be obtained within a reasonable time were unsuccessful. Flow rate values exceeded 1.23×10^{-2} std. cc/sec cm^2 for both elevated temperatures. It is known that hydrogen dissolves in platinum in large volumes and cannot be readily removed by vacuum treatment or heating, and this may offer a partial explanation. Refer to Appendix A to determine how flow rate values were computed. Since only one point was obtained, it was impossible to plot a curve for hydrogen. The trend appears to be a rising flow rate with an increase in temperature.

The xenon flow rate increased steadily with an increase in temperature, but the increase was not nearly as rapid as that observed with the helium.

In comparing the flow rates of the helium with the xenon, it is noted that the xenon had a higher flow rate at 500°C (773°K) but because the rate increased at a lower rate than the helium, at elevated temperatures, the filter becomes more selective in passing xenon; thus at 500°C (773°K) the He:Xe ratio is 0.658 Xe while at 850°C and 1050°C (1123° and 1323°K) the ratio has become 82.2 Xe and 131.5 Xe, respectively.

When the 50:50:1 gas mixture is examined, the same phenomena as observed above occurs but is more pronounced since the partial pressures are 50:1 instead of 1:1. Again, the hydrogen flow values are unobtainable because of RGA sensitivity.

As mentioned earlier, the expected flow at a given temperature and pressure for the gases was greatest for helium, hydrogen next and xenon least. The reasoning for this expectation is based upon the cross-sectional areas of the gases involved. The hydrogen atom has a diameter of 0.77 angstoms (Å) (77×10^{-2} m) but since it is diatomic, the distance between atoms becomes 2.75 Å (2.75×10^{-10} m). For helium, the atomic diameter is 1.86 Å (1.86×10^{-10} m) and for xenon 3.80 Å (3.80×10^{-10} m); yet at 500°C (773°K) both xenon and hydrogen had a greater flow rate than helium through Filter #307. No explanation can be offered for this phenomena.

Filter #319 was tested after #307. Upon completion of the room temperature helium flow test, the elevated temperature tests were started and data were obtained for helium at 500 and 850°C (773 and 1123°K). At 1050°C (1373°K) the RGA registered no gas flow. The system was pumped out and repressurized to 100 psia (6.89×10^5 N/m^2) but there was still no flow. The filter was cooled to room temperature and repressurized to 200 psia (1.38×10^6 N/m^2) with helium and again no flow was indicated. It was concluded that the filter was blocked and in the light of earlier developments the blockage was probably caused by contamination from cracked diffusion pump oil.

Filter #312 had been partially tested for helium at room temperature several weeks before the trouble with the RGA pumping system occurred; however, it was not tested in 20 psi increments as required so it was retested after Filter #319 had blocked up. Upon completion of the room temperature helium flow tests, several problems arose. The filament of the Vee tube of the RGA burned out and required replacement. Then it was found impossible to obtain a pressure lower than 10^{-4} torr (1.33×10^{-2} N/m^2) in the downstream side of the filter. The pumping station was found to be contaminated due to overheating of the diffusion pump caused by a blockage of the cooling water supply. The pumping station was dismantled, thoroughly cleaned and calibrated prior to testing of additional filters. The blocking of Filter #319, the burnout of the Vee tube filament and the possible erroneous flow data for Filter #312 were attributed to the contaminated pumping system.

The flow data for Filter #312 obtained just prior to the pumping system overhaul was suspect because the flow rate was not increasing with increasing pressure indicating that it was probably blocking up. After the pump was overhauled and calibrated, Filter #312 was retested with helium at room temperature and the data reproduced that obtained several weeks earlier. The early data plus that obtained after system cleanup were used to plot the flow rate versus pressure of Filter #312 in Figure 20.

When Filter #312 was tested at elevated temperature, several anomalies arose which were inconsistent with what was expected. The flow rates for helium and hydrogen both individually and as mixed gases appear to increase in flow from 500 to 850°C (773 to 1123°K), then decrease in

flow from 850 to 1050°C (1123 to 1323°K). The flow for xenon alone steadily decreased with an increase in temperature while the mixed gas xenon behaved similarly to the hydrogen and helium mixed gases. The anomalies are unexplainable at this time. Two flow values for helium and three flow values for hydrogen exceeded the capacity of the RGA so definite flow values could not be calculated. The flow values obtained for these gases can only show trends based on the data that could be calculated.

A possible explanation for the observed increase, then decrease in flow with increasing temperature, could be due to blockage of vent pores due to diffusion of platinum or volatilization and deposition of chromium from the Haynes 25. The vents were diffusion bonded with platinum into Haynes 25 housings by heating for 76 hours (2.74×10^5 s) at 760°C (1033°K). The two higher test temperatures of 850 and 1050°C (1123 and 1323°K) were above the diffusion bonding temperature of the platinum so some additional diffusion of platinum could be expected at the test temperatures. The diffused platinum could reduce some of the cross-sectional area of the filter thereby reducing gas flow. Chromium is known to volatize from Haynes 25 at elevated temperature and low pressure.

The filter vents were subjected to several thermal cycles during the elevated temperature tests. These occurred as a result of the testing schedule employed. The schedule was as follows: After testing at room temperature, heat to 500°C (773°K) in about four hours (14.4×10^3 s), test for helium, hydrogen, xenon and mixed gases flow rate, evacuate system and maintain at 500°C (773°K) overnight. In the morning, heat to 850°C (1123°K) in about four hours (1.44×10^3 s) and retest for gas flow rates, evacuate system and cool to 500°C (773°K) overnight. The following morning reheat to 1050°C (1323°K) in about four hours (1.44×10^3 s) and retest for gas flow rates, evacuate system and cool to room temperature.

This thermal cycling could possibly affect flow rates because of the differences in thermal expansion of the filter materials and the Haynes 25 housings. A comparison of the thermal expansions at the test temperatures of the various materials employed is given below.

Thermal Expansion, $X10^{-6}/°K$

	Haynes 25	Lucalox	ZrO_2
500°C (773°K)	14.4	7.7	12.1
850°C (1123°K)	16.3	8.1	15.3
1050°C (1323°K)	16.9	8.5	15.3

The Haynes 25 housing expands at a greater rate than either of the vent materials. This would tend to put the platinum bond into tension at elevated temperatures. The effect would be more severe with Lucalox than

ZrO_2 because of the greater expansion differences. At room temperature all vents are under compression because the filter is installed with a 0.0002 inch (5.08×10^{-6} m) interference fit.

As the filter heats, both the housing and the filter expand with the housing expanding at a faster rate until at some temperature the compressive stress is zero after which the stress goes into tension. If the tensile stress is great enough, the bond between the vent and the housing may rupture permitting gross flow; however, no gross flow was noted in our tests. As the initial compressive stresses become relieved during heating, an increase in flow is anticipated because of pore or void enlargement.

Another possible source of unanticipated vent contamination with possible detrimental effects might be from the test gas impurities. The xenon gas was research grade and had a minimum purity of 99.995% and listed dew point of -110°F (203°K). The hydrogen and helium gases were welding grade purity (99.9%) with listed dew points of -70°F (228°K). Actual dew points on the test gases were not taken because this was not considered a critical factor at that time. Yet, if oxygen or water vapor were present even in minute amounts, these impurities could react with the Haynes 25 housing which, in turn, would contaminate the filter.

The flow characteristics for most of the gases tested appeared to be an increase in flow probably due to thermal expansion followed by a decrease in flow probably due to blockage of pores by diffusion of platinum or volatilization of chromium or contamination by impure gases or other unknown causes. Flow rate curves for the pure and mixed helium and hydrogen gases could not be plotted because of the unknown flow values obtained when the RGA flooded. The xenon did not flood the RGA but produced two flow curves that are anomalous; i.e., one increases with temperature while the other decreases with temperature. No explanation can be given for this behavior.

Filter #323 was tested next and the flow data again was anomalous. This time the helium and xenon flow rates increased, then decreased with an increase in temperature, while the hydrogen decreased steadily with temperature. The order of selectivity was helium with the greatest flow rate followed by xenon and hydrogen least flow. These results were not in accord with what was expected in view of the results obtained with earlier test filters. Six data points were unknown since the capacity of the RGA was exceeded and occurred with the same gases, helium at 850°C (1123°K) and hydrogen at 850 and 1050°C (1123 and 1323°K) for both the pure and mixed gases.

Filter #316 was anomalous in all respects. The pure helium flow decreased, then increased with an increase in temperature; the hydrogen indicated no flow at one data point, yet had flow at the next data point

while the xenon increased three magnitudes in flow rate over the temperature range investigated. The mixed gas data were equally anomalous. The helium flow decreased steadily with temperature three magnitudes, the hydrogen increased, then decreased with an increase in temperature, while the xenon decreased, then increased with an increase in temperature. Three data points were unknown since in two cases the RGA capacity was exceeded, while in the third case no flow was indicated. It is not known how the order of testing gases affects the flow behavior through a filter or the sensing filament of the RGA, but it is possible that the elevated temperature results obtained may have been affected by the change from one gas to another during testing.

Filter #351 was tested only with helium and hydrogen at elevated temperatures because the xenon supply was exhausted by the time this filter was tested. The data show very little selectivity of the filter to these gases and the flow rates were high in comparison with those obtained with the other filters (10^{-1} cc/sec versus 10^{-4} to 10^{-7} cc/sec).

In reviewing the flow data for the six filters tested, one notes that the room temperature helium flow rates were consistent. The flow rates increased fairly uniformly with an increase in pressure, appeared to increase with a decrease in filter density, and increased with increase in filter diameter and decrease in L/D ratio.

However, the elevated temperature flow data for helium, hydrogen, xenon and a 50:50:1 mixture of these same gases presented many anomalies which cannot be readily explained with the available data. The anomalies are of such a nature that one must conclude that the elevated temperature flow data cannot be used to reach conclusions for the gases tested. Since hydrogen and xenon gases had never been tested previously, either at room or elevated temperatures, one could only anticipate what the flow behavior should be. Unfortunately, the data obtained were so anomalous no trends were indicated and the observed flow behavior was not anticipated.

The elevated temperature anomalies are attributed to some or all of the points discussed earlier in this report. These included:

1. Inability to obtain a definite flow value because the capacity of the RGA was exceeded during testing. Lack of data points (only three were taken) prevented plotting of representative curves.

2. Possible contamination of filters by impurities in the test gases.

3. Thermal expansion differences between housing and filter vent materials which could lead to paradoxical flow behavior at elevated temperatures.

4. Diffusion of the platinum used to bond the filter to the housing during the elevated temperature tests which decreased the area of the filter.

5. Absorption of hydrogen by platinum.

6. Volatilization of the Haynes 25 housing material at temperature which could subsequently block vent pores.

7. Thermal cycling of vents due to the inability to test a given filter at the required test conditions in a working day without interruption.

8. Possible changes in vent flow characteristics resulting from changing test gases frequently.

9. Possible changes in the RGA due to changes in test gases.

In order to minimize the foregoing problems in future work, the following steps should be observed.

1. Determine six to eight data points so that if a data point is unobtainable a general curve can still be drawn.

2. Attempt to match thermal expansions of the housing and vent materials.

3. Use a bonding material which does not diffuse or adsorb the test gases at temperature.

4. Change the housing to a material that is more stable under these severe conditions.

5. Do not thermally cycle vents during test.

6. Purify test gases before admitting to test system.

7. Test a filter with one gas, test a duplicate filter with a different gas, then interchange filters and test. Finally, repeat original tests to see if flow rates are altered significantly.

8. Test all gases at room temperature prior to elevated temperature tests.

9. Retest all filters at room temperature to determine if flow rates are altered by elevated temperature tests.

SUMMARY OF RESULTS

Flame sprayed Al_2O_3 and ZrO_2 coatings were evaluated as protective barrier coatings on tantalum metal. Both coatings were bent 180° over a 1/2 inch (1.27×10^{-2}m) diameter mandrel. The Al_2O_3 coating spalled on both the exterior and interior of the bend, while the ZrO_2 coating spalled only on the interior.

The same coatings were exposed to a 3 weight percent lithium pentaborate solution for 500 (1.8×10^6 sec) and 1000 (3.6×10^6 sec) hours at 150°C (423°K). Both coatings were intact after the test with no evidence of spalling, cracking, blistering or peeling. The tantalum substrate was sound with no evidence of attack by the pentaborate solution.

Simulated reactor fuel was melted and dropped onto Al_2O_3 and ZrO_2 coated tantalum cups. Three fuel formulations were melted, namely, Type 304 stainless steel, an equal weight mixture of depleted UO_2-Mo, and an equal weight mixture of Type 304 stainless steel, depleted UO_2 and Mo. Some cracking of the coating occurred, but both coatings were effective in preventing a reaction between the molten fuel and the tantalum substrate since the fuel solidified before it could penetrate the cracks in the coating.

Two coated cups with molten SS-UO_2-Mo fuel in them were tested in wet hydrogen at elevated temperature. The fuel did not react with the ZrO_2 coating but did react with the Al_2O_3 coating at the test temperature.

Six filter vents were fabricated and tested for selectivity in venting hydrogen, helium, xenon and a mixture of these gases at various temperatures and pressures. The effects of material, material density, geometry, gas temperature, gas pressure, and gas molecular size upon flow rate were investigated. The materials tested were Al_2O_3 and ZrO_2 in two different densities, two different geometries, at three different temperatures, and gas pressures ranging from 20 to 200 PSIA (1.38×10^5 N/m^2 to 1.38×10^6 N/m^2). The gases tested were hydrogen, helium, xenon and a mixture of these gases. The room temperature helium flow tests indicated that flow rates can be varied. The flow rates increased with decreasing material density, with increased gas backpressures, and increased filter surface area with decreased length. Conclusions could not be made concerning flow rates of helium, hydrogen, xenon and mixtures of these gases at elevated temperatures because of anomalous data. However, it can be concluded that in the present state of development these filters are not directly applicable to venting the gases desired at elevated temperatures.

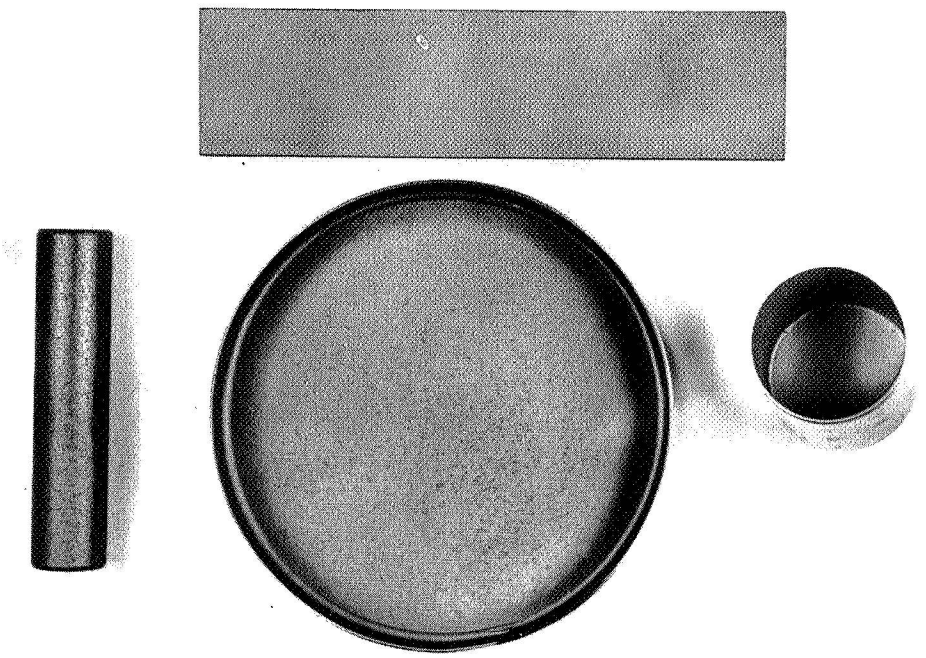

FIG. 1. TANTALUM CONTAINMENT VESSELS AND SPECIMENS BEFORE COATING

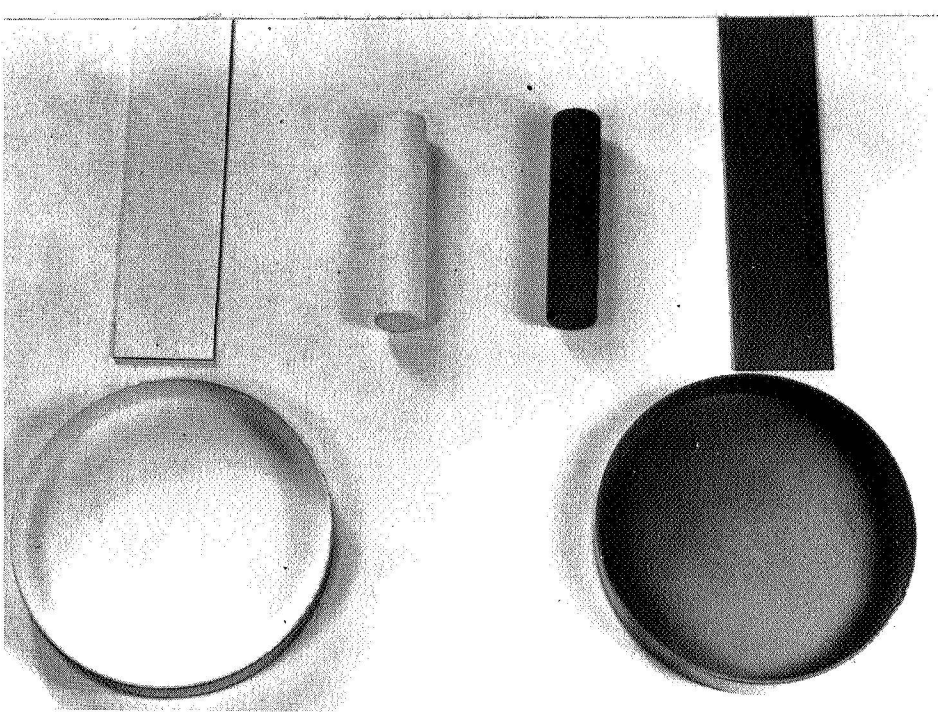

FIG. 2. TANTALUM CONTAINMENT VESSELS AND SPECIMENS AFTER COATING, Al_2O_3 COATING ON LEFT

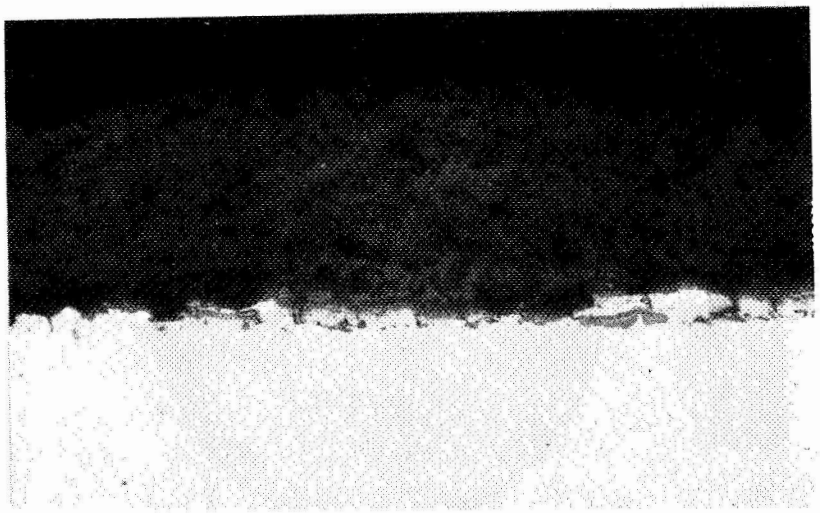

FIG. 3. METALLOGRAPHIC SECTION OF Al_2O_3 COATED COUPON AS SPRAYED AND HEAT TREATED

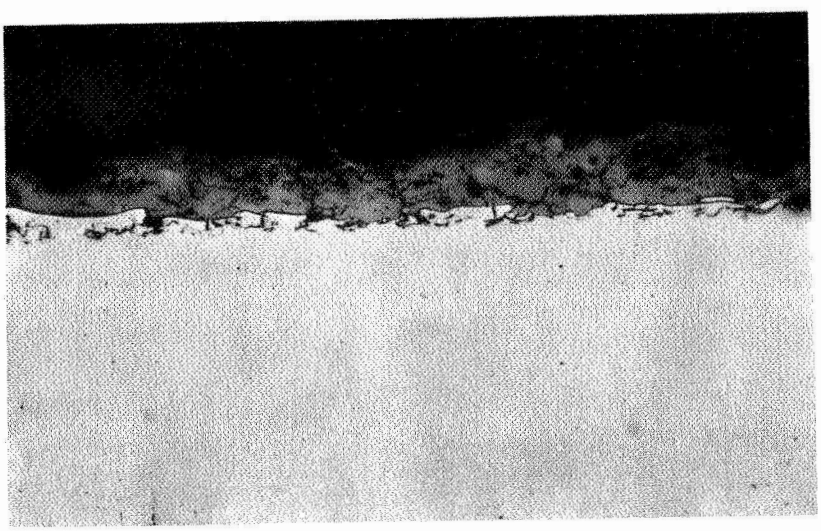

FIG. 4. METALLOGRAPHIC SECTION OF ZrO_2 COATED COUPON AS SPRAYED AND HEAT TREATED

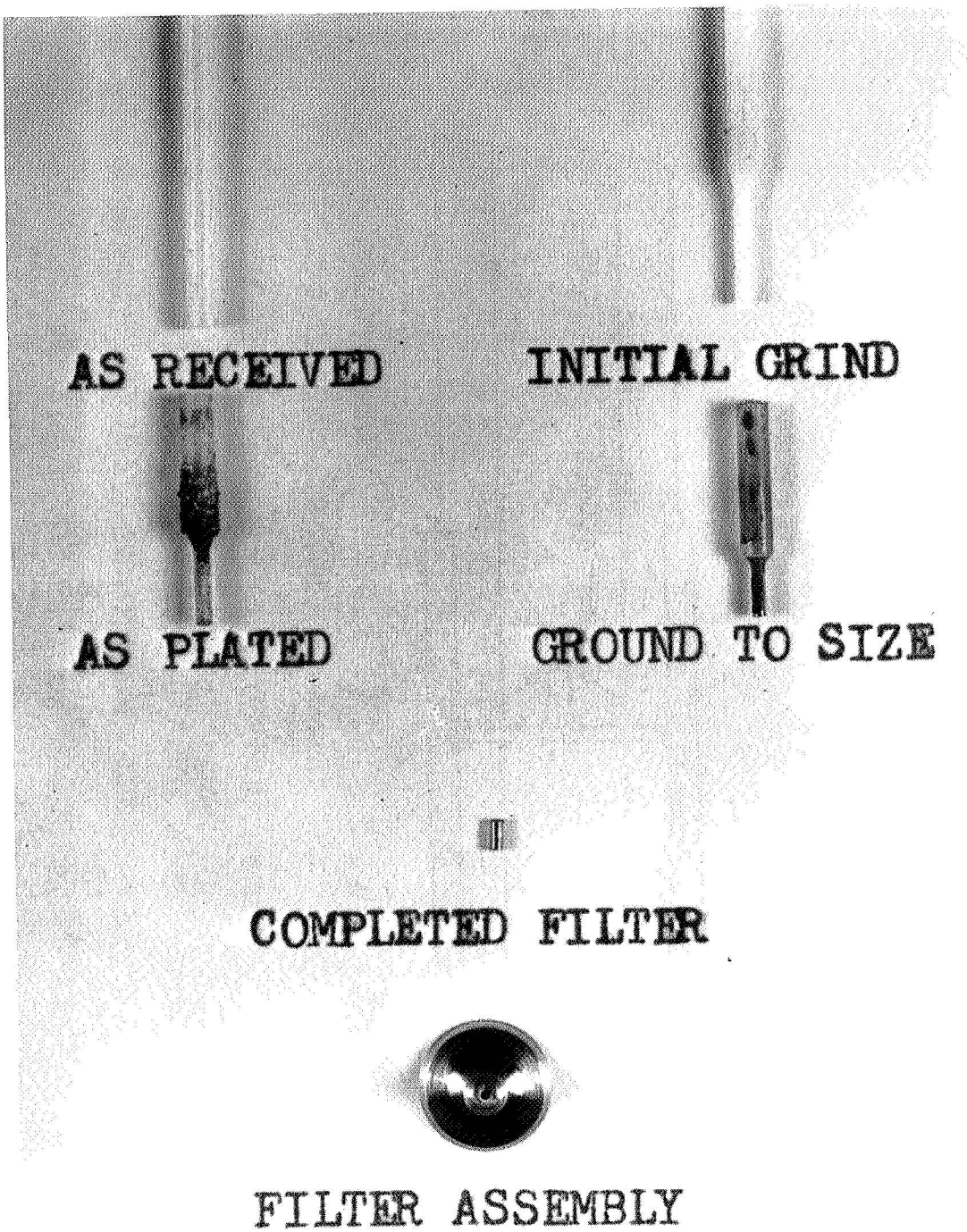

FIG. 5. PROCESSING OF FILTER VENT ELEMENTS

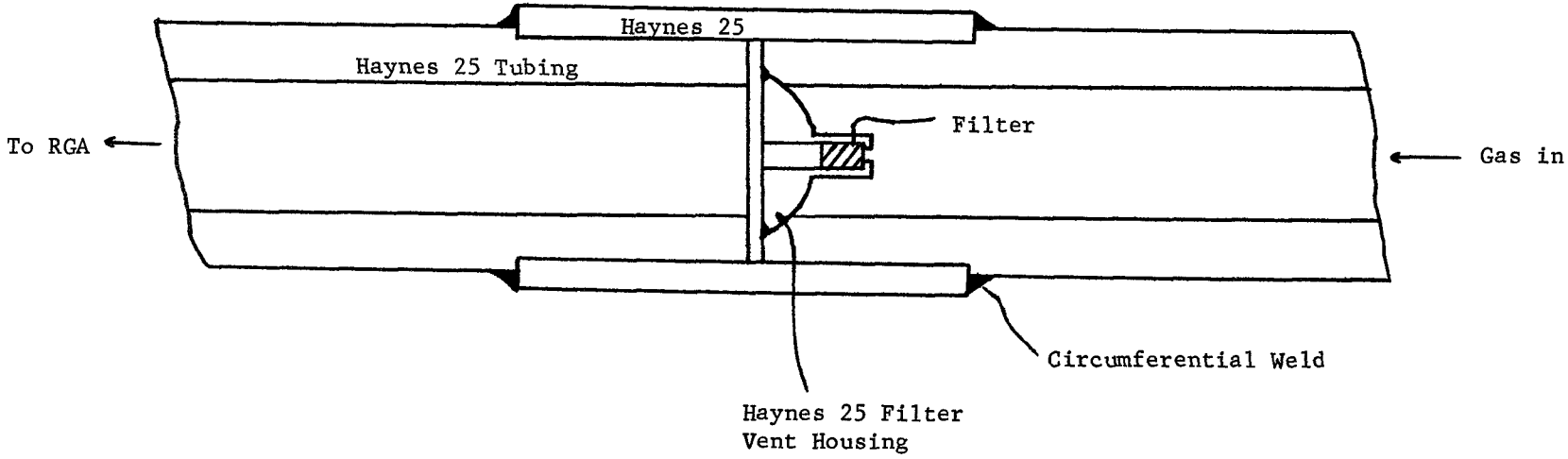

FIG. 6. FILTER VENT TEST FIXTURE

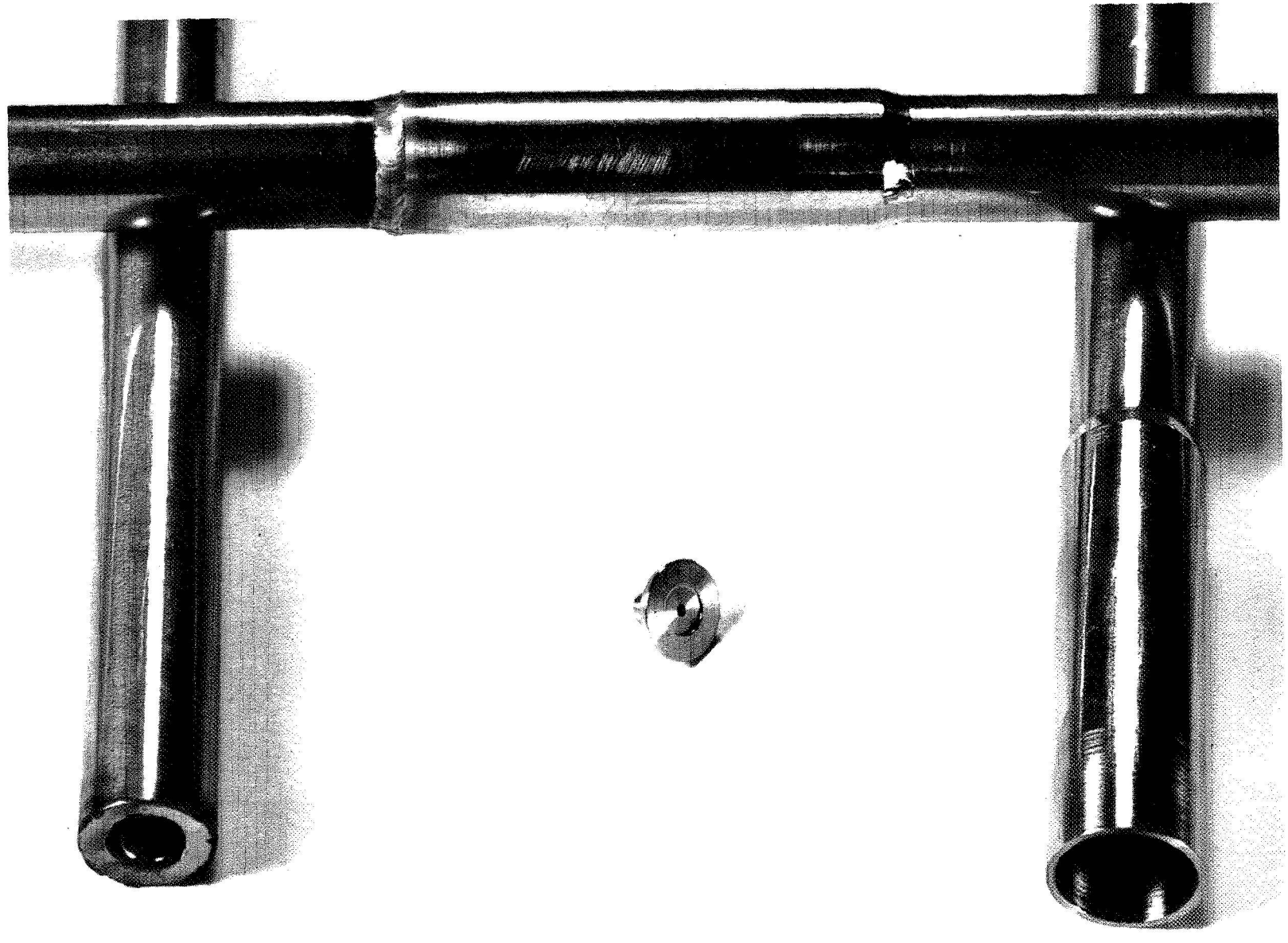

FIG. 7. FILTER VENT ASSEMBLY

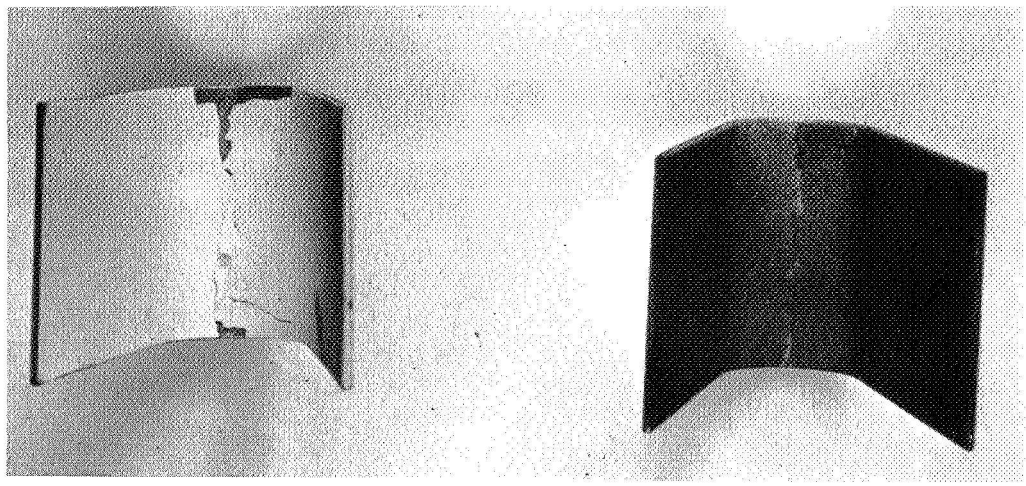

FIG. 8. INTERIOR BEND OF COATED COUPONS, Al_2O_3 ON LEFT

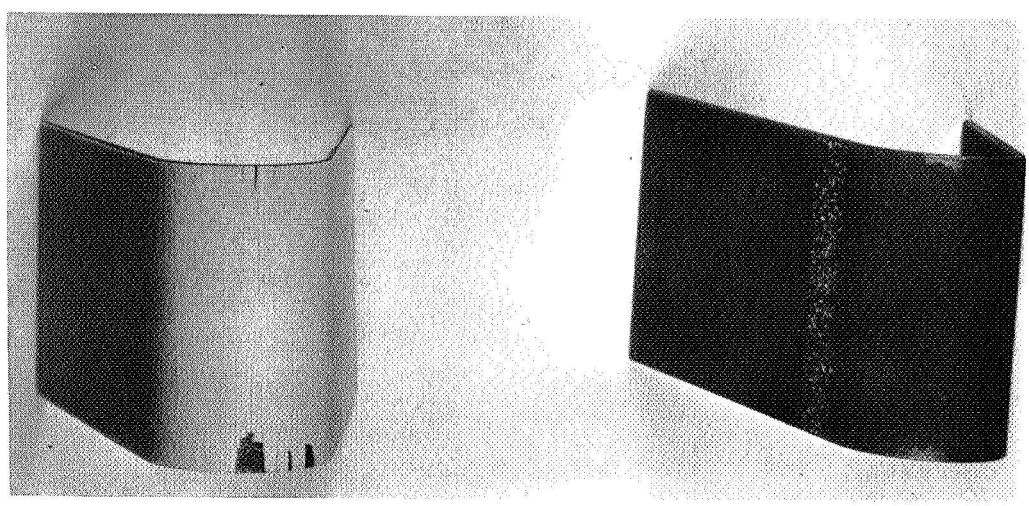

FIG. 9. EXTERIOR BEND OF COATED COUPONS, Al_2O_3 ON LEFT

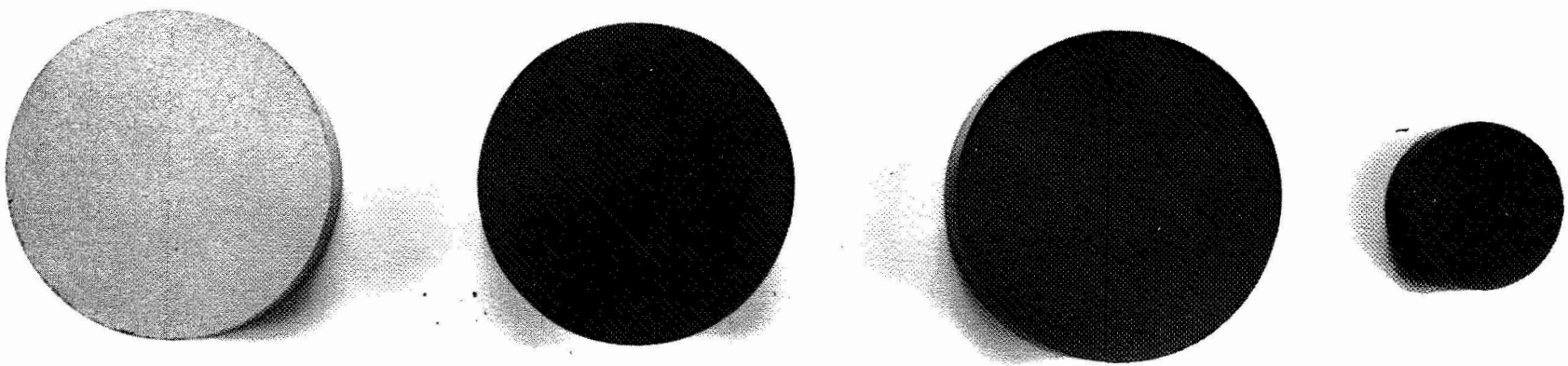

S/S

Mo-UO_2

S/S-Mo-UO_2

S/S-Mo-UO_2

FIG. 10. SIMULATED FUEL PELLETS

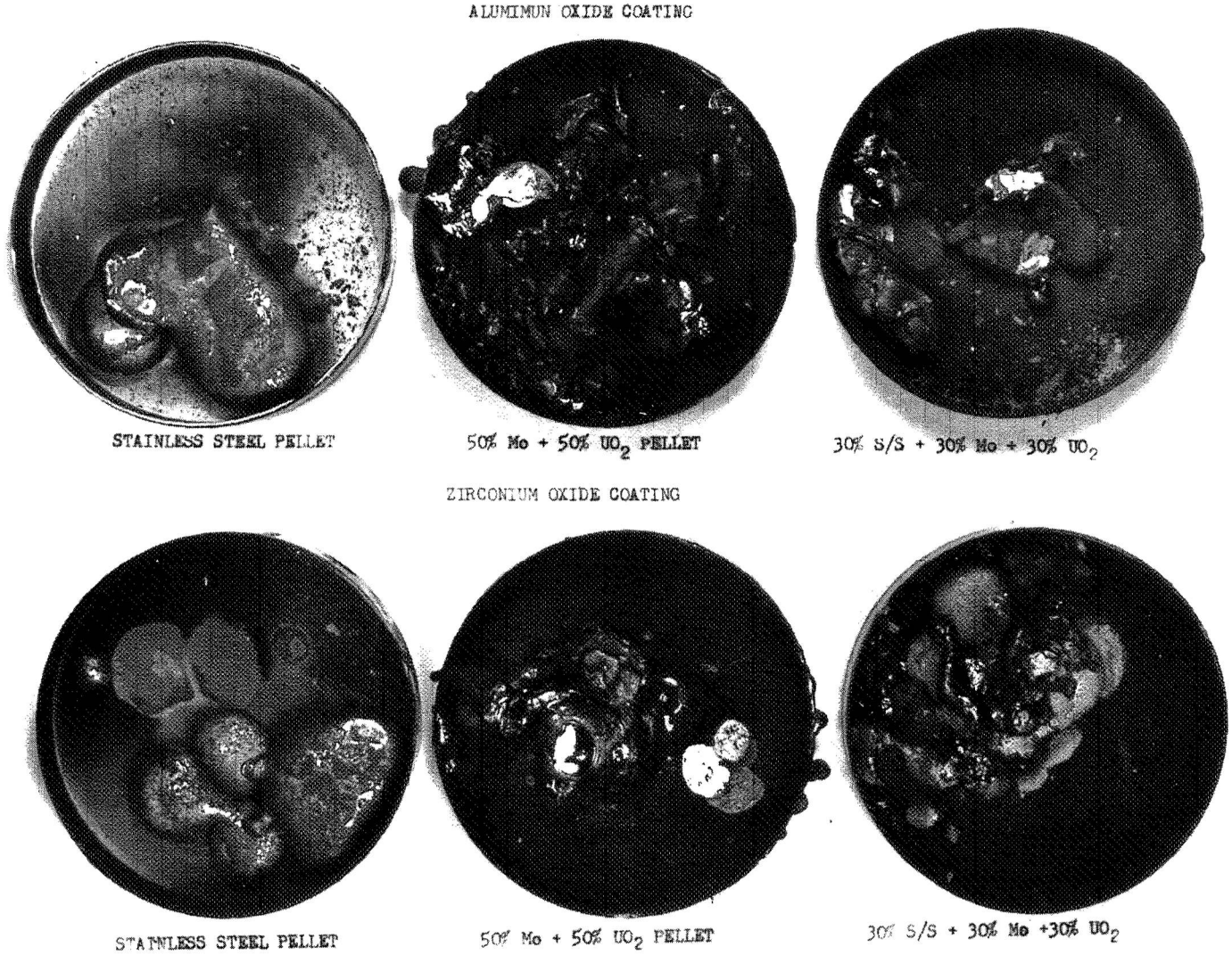

FIG. 11. APPEARANCE OF CONTAINMENT VESSELS AFTER MELTDOWN

METALLOGRAPHIC SECTIONS - 250X
APPEARANCE OF Al_2O_3 OR ZrO_2 COATING ON TANTALUM AFTER MELTDOWN TEST

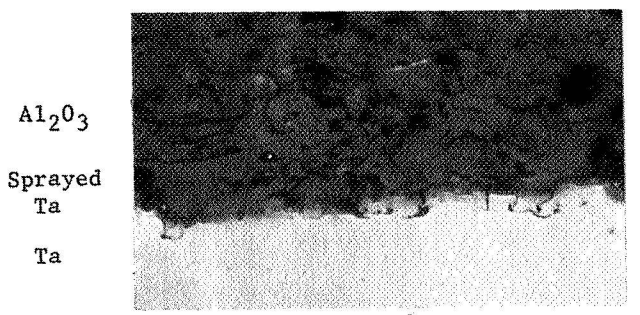

FIG. 12. STAINLESS STEEL ON Al_2O_3

FIG. 13. STAINLESS STEEL ON ZrO_2

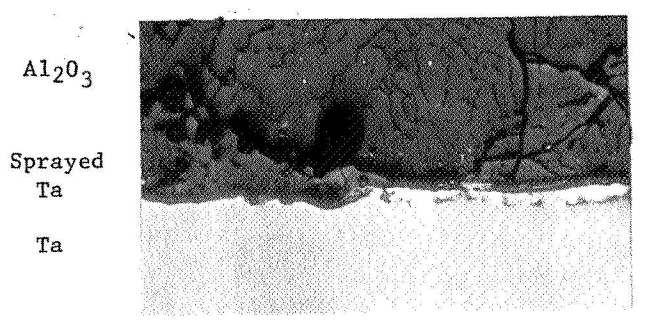

FIG. 14. Mo-UO_2 on Al_2O_3

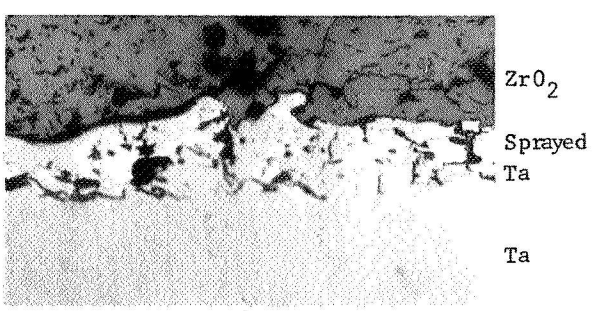

FIG. 15. Mo-UO_2 on ZrO_2

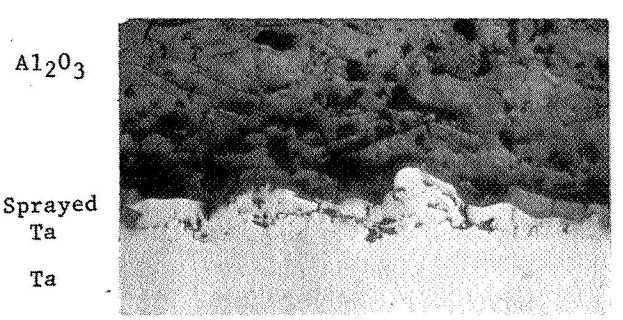

FIG. 16. STAINLESS STEEL-Mo-UO_2 ON Al_2O_3

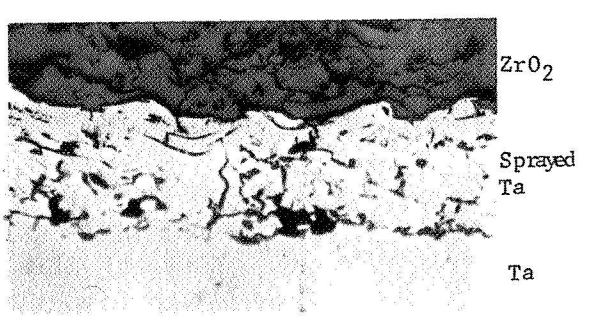

FIG. 17. STAINLESS STEEL-Mo-UO_2 ON ZrO_2

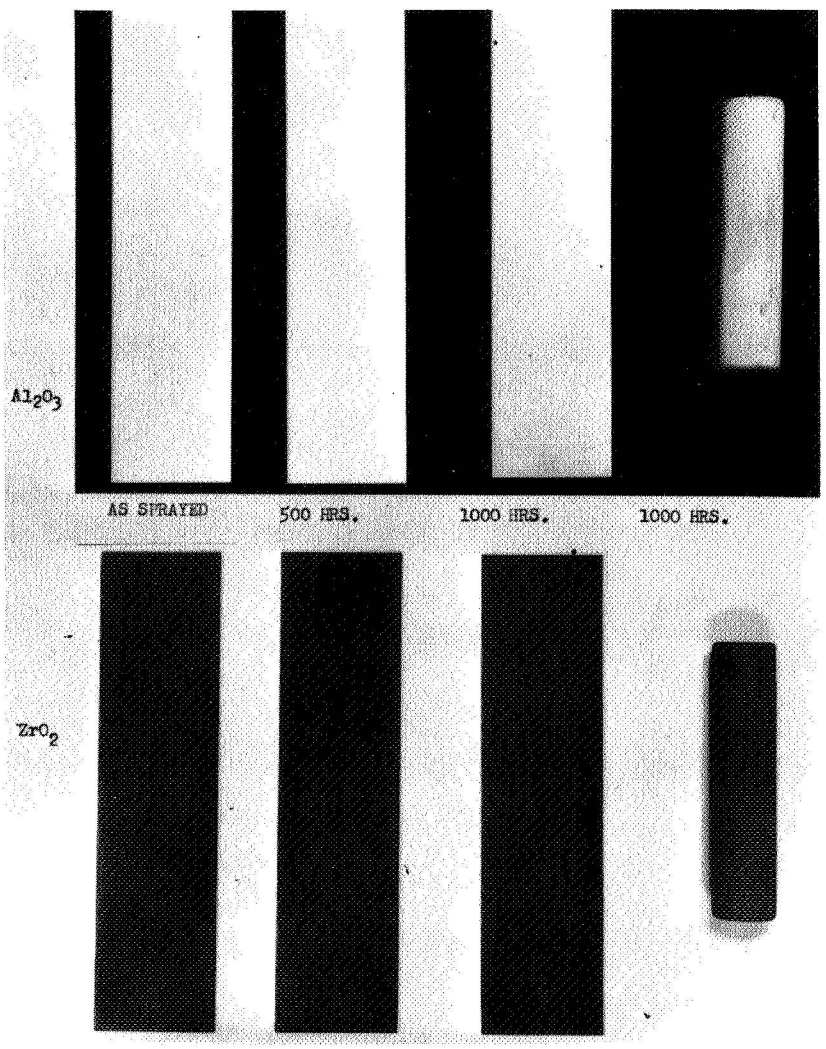

FIG. 18. COATED SPECIMENS AFTER SPRAYING AND AFTER 500 and 1000 HOURS IN LITHIUM PENTABORATE

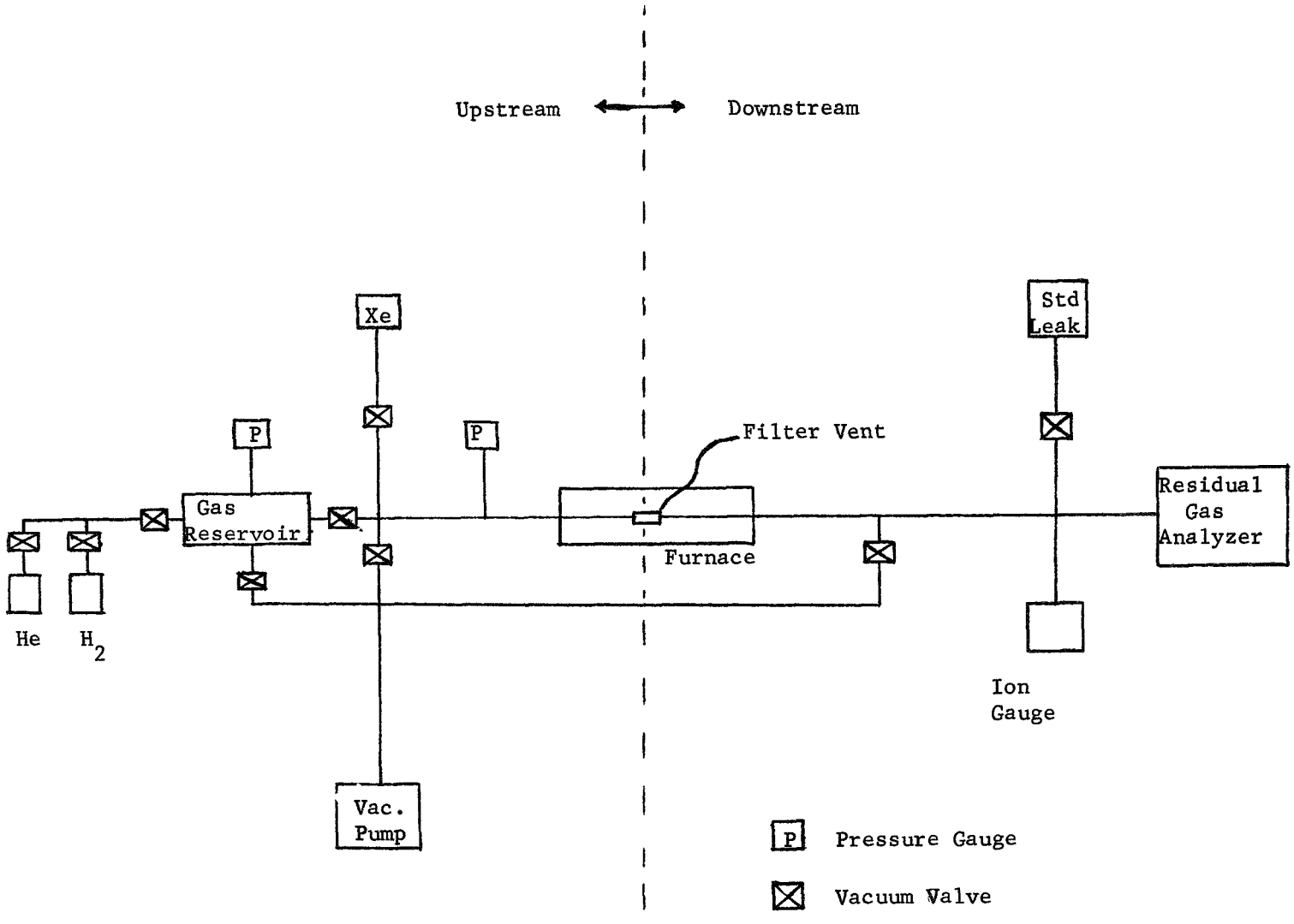

FIG. 19. FILTER VENT TEST CONSOLE FLOW DIAGRAM

FIG. 20 ROOM TEMPERATURE HELIUM FLOW RATES
FLOW RATE VERSUS PRESSURE

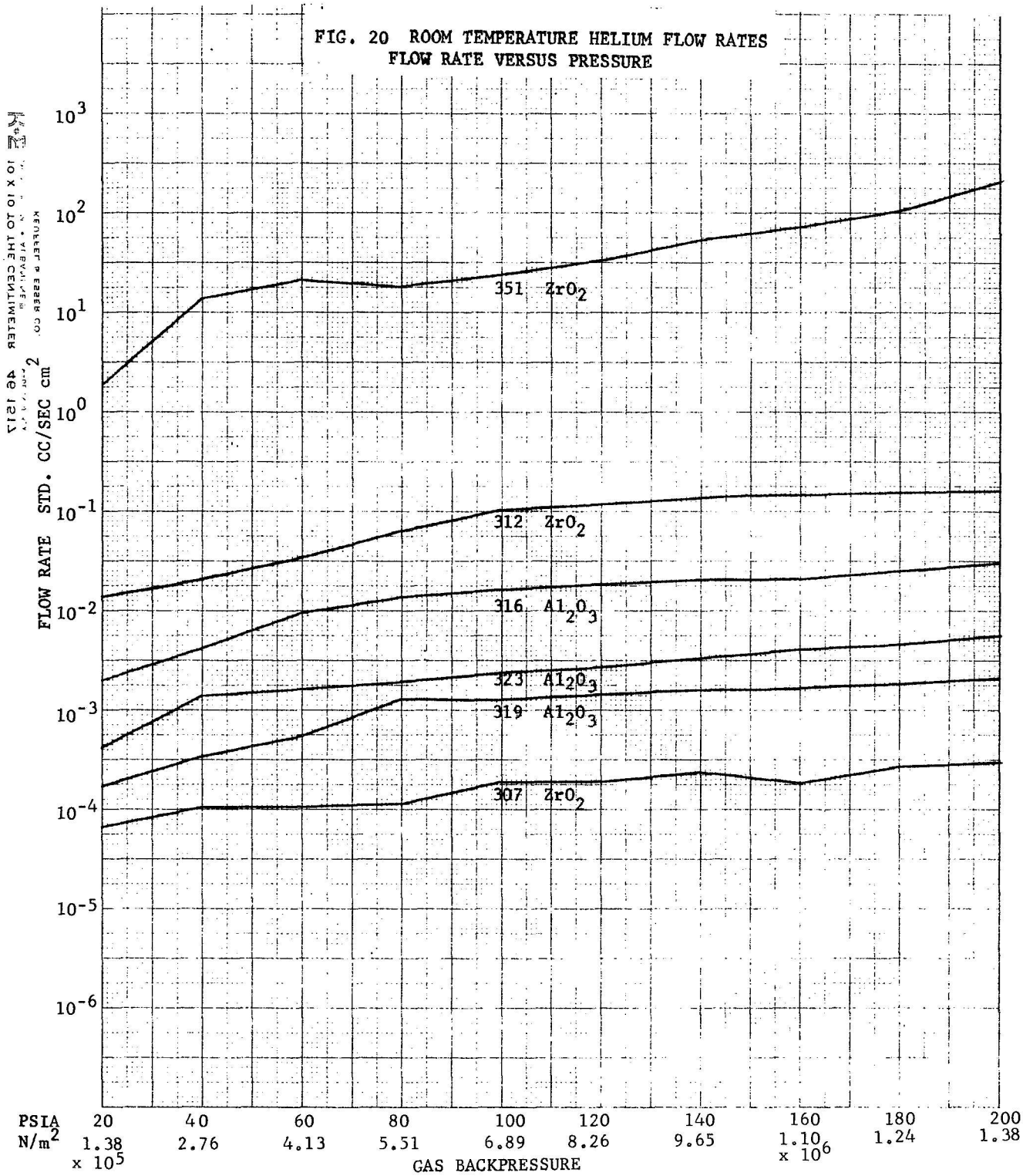

TABLE I

FILTER VENT IDENTIFICATION

Order Tested	Haynes 25 Housing Number	Hole Diameter Inches	Hole Diameter (m)	Material Installed Material	Diameter X Length Inches	Diameter X Length (m)	Assembly Number
1	307	0.0398	1.01×10^{-3}	ZrO_2 5.71*	0.0401 x 0.0904	1.02×10^{-3} by 2.30×10^{-3}	307/9A
3	312	0.0779	1.98×10^{-3}	ZrO_2 5.71	0.0785 x 0.0451	1.99×10^{-3} by 1.15×10^{-3}	312/4
5	316	0.0781	1.98×10^{-3}	Al_2O_3 3.98	0.0785 x 0.0448	1.99×10^{-3} by 1.14×10^{-3}	316/1
2	319	0.0398	1.01×10^{-3}	Al_2O_3 3.93	0.0401 x 0.0907	1.02×10^{-3} by 2.30×10^{-3}	319/13
4	323	0.0397	1.01×10^{-3}	Al_2O_3 3.93	0.0401 x 0.0901	1.02×10^{-3} by 2.29×10^{-3}	323/20
6	351	0.0399	1.01×10^{-3}	ZrO_2 3.80	0.0401 x 0.0890	1.02×10^{-3} by 2.26×10^{-3}	351/333

* 5.71 density in grams/cc

TABLE II

ROOM TEMPERATURE HELIUM FLOW RATES FOR FILTER 307/9A

ZrO_2 0.040 inch O.D. x 0.090 inch Long (1.02×10^{-3}m by 2.29×10^{-3}m)

Cross-Sectional Area = 8.1×10^{-3} cm^2, Density 5.71 gm/cc, L/D = 2.25

Source Pressure		Helium Gas	
PSIA	(N/m^2)	std cc/sec	std cc/sec-cm^2
20	1.38×10^5	6.7×10^{-8}	8.24×10^{-6}
40	2.76×10^5	1.03×10^{-7}	1.27×10^{-5}
60	4.13×10^5	1.07×10^{-7}	1.32×10^{-5}
80	5.51×10^5	1.27×10^{-7}	1.56×10^{-5}
100	6.89×10^5	2.38×10^{-7}	2.93×10^{-5}
120	8.26×10^5	2.38×10^{-7}	2.93×10^{-5}
140	9.65×10^5	3.17×10^{-7}	3.90×10^{-5}
160	1.10×10^6	2.17×10^{-7}	2.67×10^{-5}
180	1.24×10^6	3.56×10^{-7}	4.38×10^{-5}
200	1.38×10^6	3.96×10^{-7}	4.87×10^{-5}

TABLE III

FLOW RATES FOR FILTER 307/9A

ZrO_2 0.040 inch O.D. x 0.090 inch long (1.02×10^{-3} m by 2.29×10^{-3} m)

Cross-Sectional Area = 8.1×10^{-3} cm^2, Density 5.71 gm/cc, L/D = 2.25

				Mixed Gases He, H_2, Xe (50:50:1)		
Gas	Helium	Hydrogen	Xenon	Helium	Hydrogen	Xenon
Source Pressure						
PSIA	100	100	100	50	50	1
N/m^2	6.89×10^5	6.89×10^5	6.89×10^5			
Temperature						
500°C (773°K)						
Std cc/sec	1.1×10^{-6}	4.56×10^{-6}	1.67×10^{-6}	2.34×10^{-5}	5.17×10^{-7}	1.80×10^{-7}
Std cc/sec-cm^2	1.35×10^{-4}	5.61×10^{-4}	2.05×10^{-4}	2.88×10^{-3}	6.36×10^{-5}	2.21×10^{-5}
Ratio						
He =			.658 Xe			1.30 Xe
H_2 =	4.156 He		2.74 Xe	.0221 He		2.88 Xe
Xe =	1.518 He			.008 He		
850°C (1123°K)						
Std cc/sec	1.21×10^{-3}	$>1.0 \times 10^{-4}$	1.48×10^{-5}	7.38×10^{-5}	$>1.0 \times 10^{-5}$	4.18×10^{-6}
Std cc/sec-cm^2	1.48×10^{-1}	$>1.23 \times 10^{-1}$	1.82×10^{-3}	9.08×10^{-3}	$>1.0 \times 10^{-2}$	5.14×10^{-5}
Ratio						
He =			82.2 Xe			.177 Xe
H_2 =	>.0831 He		>6.76 Xe	>.110 He		>19.5 Xe
Xe =	.0123 He			.006 He		
1050°C (1323°K)						
Std cc/sec	2.3×10^{-3}	$>1.0 \times 10^{-4}$	1.73×10^{-5}	5.60×10^{-4}	$>1.0 \times 10^{-5}$	1.67×10^{-6}
Std cc/sec-cm^2	2.80	$>1.23 \times 10^{-1}$	2.13×10^{-3}	6.89×10^{-2}	$>1.0 \times 10^{-2}$	2.05×10^{-5}
Ratio						
He =			131.5 Xe			3360 Xe
H_2 =	>.0439 He		>5.77 Xe	>.0145 He		>48.8 Xe
Xe =	.0076 He			.0003 He		

TABLE IV

ROOM TEMPERATURE HELIUM FLOW RATES FOR FILTER 319/13

Al_2O_3 0.040 inch O.D. x 0.090 inch Long (1.02×10^{-3}m by 2.29×10^{-3}m)
Cross-Sectional Area = 8.1×10^{-3} cm^2, Density 3.93 gm/cc, L/D = 2.25

Source Pressure		Helium Gas	
PSIA	(N/m^2)	Std cc/sec	Std cc/sec-cm^2
20	1.38×10^5	1.93×10^{-7}	2.37×10^{-5}
40	2.76×10^5	4.40×10^{-7}	5.41×10^{-5}
60	4.13×10^5	6.05×10^{-7}	7.44×10^{-5}
80	5.51×10^5	9.35×10^{-7}	1.15×10^{-4}
100	6.89×10^5	9.35×10^{-7}	1.15×10^{-4}
120	8.26×10^5	1.38×10^{-6}	1.70×10^{-4}
140	9.65×10^5	1.65×10^{-6}	2.03×10^{-4}
160	1.10×10^6	1.87×10^{-6}	2.30×10^{-4}
180	1.24×10^6	2.09×10^{-6}	2.57×10^{-4}
200	1.38×10^6	2.64×10^{-6}	3.25×10^{-4}

TABLE V

FLOW RATES FOR FILTER 319/13

Al_2O_3 0.040 inch O.D. x 0.090 inch long (1.02×10^{-3} by 2.29×10^{-3}m)

Cross-Sectional Area = 8.1×10^{-3} cm^2, Density 3.93 gm/cc, L/D = 2.25

				Mixed Gases He, H_2, Xe (50:50:1)		
Gas	Helium	Hydrogen	Xenon	Helium	Hydrogen	Xenon
Source						
Pressure						
PSIA	100					
N/m^2	6.89×10^5					
Temperature						
500°C (773°K)						
Std cc/sec	1.68×10^{-6}	Filter	Filter	Filter		
Std cc/sec-cm^2	2.07×10^{-4}	Blocked	Blocked	Blocked		
Ratio						
He =						
H_2 =						
Xe =						
850°C (1123°K)						
Std cc/sec	1.0×10^{-5}					
Std cc/sec-cm^2	1.23×10^{-3}					
Ratio						
He =						
H_2 =						
Xe =						
1050°C (1373°K)						
Std cc/sec	Filter Blocked					
Std cc/sec-cm^2						
Ratio						
He =						
H_2 =						
Xe =						

TABLE VI

ROOM TEMPERATURE HELIUM FLOW RATES FOR FILTER 312/4

ZrO_2 0.078 inch O.D. x 0.045 inch Long (1.98×10^{-3}m by 1.14×10^{-3}m)
Cross-Sectional Area = 3.1×10^{-2} cm^2, Density 5.71 gm/cc, L/D = 0.56

Source Pressure		Helium Gas					
		New Data		Old Data		New Data After System Cleanup	
PSIA	(N/m^2)	Std cc/sec	Std cc/sec-cm^2	Std cc/sec	Std cc/sec-cm^2	Std cc/sec	Std cc/sec-cm^2
20	1.38×10^5	4.3×10^{-4}	1.4×10^{-2}			4.46×10^{-4}	1.43×10^{-2}
25	1.72×10^5			6.8×10^{-4}	2.2×10^{-2}		
40	2.76×10^5	8.8×10^{-4}	2.8×10^{-2}			1.00×10^{-3}	3.20×10^{-2}
50	3.45×10^5			1.6×10^{-3}	5.1×10^{-2}		
60	4.13×10^5	1.3×10^{-3}	4.2×10^{-2}			1.70×10^{-3}	5.44×10^{-2}
80	5.51×10^5	1.7×10^{-3}	5.4×10^{-2}			2.50×10^{-3}	8.00×10^{-2}
100	6.89×10^5	2.0×10^{-3}	6.4×10^{-2}	2.9×10^{-3}	9.3×10^{-2}	3.40×10^{-3}	1.09×10^{-1}
120	8.26×10^5	2.0×10^{-3}	6.4×10^{-2}			$>3.58 \times 10^{-3}$	$>1.15 \times 10^{-1}$
140	9.65×10^5	1.8×10^{-3}	5.8×10^{-2}			$>3.58 \times 10^{-3}$	$>1.15 \times 10^{-1}$
150	1.03×10^6			5.3×10^{-3}	1.7×10^{-1}		
160	1.10×10^6	2.6×10^{-3}	8.3×10^{-2}			$>3.58 \times 10^{-3}$	$>1.15 \times 10^{-1}$
180	1.24×10^6	2.2×10^{-3}	7.0×10^{-2}			$>3.58 \times 10^{-3}$	$>1.15 \times 10^{-1}$
200	1.38×10^6	1.9×10^{-3}	6.1×10^{-2}	6.5×10^{-3}	2.1×10^{-1}	$>3.58 \times 10^{-3}$	$>1.15 \times 10^{-1}$

TABLE VII

FLOW RATES FOR FILTER 312/4

ZrO_2 0.078 inch O.D. x 0.045 inch long (1.98×10^{-3}m by 1.14×10^{-3}m)

Cross-Sectional Area = 3.1×10^{-2} cm^2, Density 5.71 gm/cc, L/D = 0156

				Mixed Gases He, H_2, Xe (50:50:1)		
Gas	Helium	Hydrogen	Xenon	Helium	Hydrogen	Xenon
Source Pressure						
PSIA	100	100	100	50	50	1
N/m^2	6.89×10^5	6.89×10^5	6.89×10^5			
Temperature						
500°C (773°K)						
Std cc/sec	3.55×10^{-3}	$>6.37 \times 10^{-6}$	7.08×10^{-5}	1.52×10^{-4}	3.89×10^{-6}	2.78×10^{-7}
Std cc/sec-cm^2	1.02×10^{-1}	$>2.04 \times 10^{-4}$	2.27×10^{-3}	4.86×10^{-3}	1.24×10^{-4}	8.90×10^{-6}
Ratio						
He =			44.93 Xe			.546 Xe
H_2 =	>.002 He		>.0899 Xe	.0255 He		13.9 Xe
Xe =	.0222 He			.0018 He		
850°C (1123°K)						
Std cc/sec	$>4.35 \times 10^{-3}$	$>3.95 \times 10^{-4}$	9.26×10^{-7}	$>4.35 \times 10^{-3}$	3.59×10^{-3}	3.93×10^{-5}
Std cc/sec-cm^2	$>1.39 \times 10^{-1}$	$>1.26 \times 10^{-2}$	2.96×10^{-5}	$>1.39 \times 10^{-1}$	1.15×10^{-1}	1.25×10^{-3}
Ratio						
He =			<4695.9 Xe			>111 Xe
H_2 =	>.0906 He		>425.7 Xe	.827 He		92 Xe
Xe =	<.00021 He			<.009 He		
1050°C (1323°K)						
Std cc/sec	$>3.92 \times 10^{-4}$	$>2.64 \times 10^{-6}$	1.2×10^{-7}	4.59×10^{-6}	$>2.89 \times 10^{-6}$	1.18×10^{-5}
Std cc/sec-cm	$>1.25 \times 10^{-2}$	$>8.45 \times 10^{-5}$	3.84×10^{-6}	1.47×10^{-4}	$>9.25 \times 10^{-5}$	3.78×10^{-4}
Ratio						
He =			<3255.2 Xe			.389 Xe
H_2 =	>.00676 He		>22.01 Xe	>.629 He		>.245 Xe
Xe =	<.0003 He			2.57 He		

TABLE VIII

ROOM TEMPERATURE HELIUM FLOW RATES FOR FILTER 323/20

Al_2O_3 0.040 inch OD x 0.090 inch long (1.02×10^{-3} m by 2.29×10^{-3} m)
Cross-Sectional Area = 8.1×10^{-3} cm^2, Density 3.93 gm/cc, L/D = 2.25

Source Pressure		Helium Gas	
PSIA	N/m^2	Std cc/sec	Std cc/sec-cm^2
20	1.38×10^5	5.01×10^{-6}	6.16×10^{-4}
40	2.76×10^5	1.19×10^{-5}	1.46×10^{-3}
60	4.13×10^5	1.71×10^{-5}	2.10×10^{-3}
80	5.51×10^5	2.31×10^{-5}	2.84×10^{-3}
100	6.89×10^5	2.99×10^{-5}	3.68×10^{-3}
120	8.26×10^5	3.64×10^{-5}	4.48×10^{-3}
140	9.65×10^5	4.32×10^{-5}	5.31×10^{-3}
160	1.10×10^6	5.06×10^{-5}	6.22×10^{-3}
180	1.24×10^6	5.45×10^{-5}	6.70×10^{-3}
200	1.38×10^6	6.17×10^{-5}	7.59×10^{-3}

TABLE IX

FLOW RATES FOR FILTER 323/20

Al_2O_3 0.040 inch O.D. x 0.090 inch long (1.02×10^{-3}m by 1.14×10^{-3}m)

Cross-Sectional Area = 8.1×10^{-3} cm^2, Density 3.93 gm/cc, L/D = 2.25

				Mixed Gases He, H_2, Xe (50:50:1)		
Gas	Helium	Hydrogen	Xenon	Helium	Hydrogen	Xenon
Source						
Pressure	100	100	100	50	50	1
PSIA	6.89×10^5	6.89×10^5	6.89×10^5			
N/m^2						
Temperature						
500°C (773°K)						
Std cc/sec	1.37×10^{-4}	5.37×10^{-6}	1.01×10^{-5}	1.24×10^{-5}	1.28×10^{-6}	3.31×10^{-5}
Std cc/sec-cm^2	1.68×10^{-2}	6.61×10^{-4}	1.24×10^{-3}	1.52×10^{-3}	1.57×10^{-4}	4.07×10^{-3}
Ratio						
He =			13.55 Xe			.373 Xe
H_2 =	.0393 He		.533 Xe	.103 He		.039 Xe
Xe =	.0738 He			2.68 He		
850°C (1123°K)						
Std cc/sec	$>4.58 \times 10^{-4}$	$>3.95 \times 10^{-6}$	9.77×10^{-5}	$>4.58 \times 10^{-4}$	$>4.64 \times 10^{-6}$	9.68×10^{-5}
Std cc/sec-cm^2	$>5.63 \times 10^{-2}$	$>4.86 \times 10^{-4}$	1.2×10^{-2}	$>5.63 \times 10^{-2}$	$>5.70 \times 10^{-4}$	1.19×10^{-2}
Ratio						
He =			4.69 Xe			4.73 Xe
H_2 =	.00863 He		.0405 Xe	.0101 He		.048 Xe
Xe =	.213 He			.211 He		
1050°C (1323°K)						
Std cc/sec	1.25×10^{-4}	$>1.86 \times 10^{-6}$	9.34×10^{-6}	6.22×10^{-5}	$>2.18 \times 10^{-6}$	3.46×10^{-5}
Std cc/sec-cm^2	1.54×10^{-2}	$>2.29 \times 10^{-4}$	1.15×10^{-3}	7.65×10^{-3}	$>2.68 \times 10^{-4}$	4.26×10^{-3}
Ratio						
He =			13.39 Xe			1.80 Xe
H_2 =	.148 He		.199 Xe	.035 He		.063 Xe
Xe =	.0747 He			.557 He		

TABLE X

ROOM TEMPERATURE HELIUM FLOW RATES FOR FILTER 316/1

Al_2O_3 0.078 inch OD x 0.045 inch long (1.98×10^{-3} by 1.14×10^{-3}m)
Cross-Sectional Area = 3.1×10^{-2} cm^2, Density 3.98 gm/cc, L/D = 0.56

Source Pressure		Helium Gas	
PSIA	(N/m^2)	Std cc/sec	Std cc/sec-cm^2
20	1.38×10^5	9.26×10^{-5}	2.96×10^{-3}
40	2.76×10^5	1.94×10^{-4}	6.20×10^{-3}
60	4.13×10^5	3.10×10^{-4}	9.92×10^{-3}
80	5.51×10^5	4.54×10^{-4}	1.45×10^{-2}
100	6.89×10^5	6.72×10^{-4}	2.15×10^{-2}
120	8.26×10^5	7.92×10^{-4}	2.53×10^{-2}
140	9.65×10^5	9.61×10^{-4}	3.07×10^{-2}
160	1.10×10^6	1.15×10^{-3}	3.68×10^{-2}
180	1.24×10^6	1.32×10^{-3}	4.22×10^{-2}
200	1.38×10^6	1.56×10^{-3}	4.99×10^{-2}

TABLE XI

FLOW RATES FOR FILTER 316/1

Al_2O_3 0.078 inch O.D. x 0.045 inch long (1.98×10^{-3} m by 1.14×10^{-3} m)

Cross-Sectional Area = 3.1×10^{-2} cm^2, Density 3.98 gm/cc, L/D = 0.56

				Mixed Gases He, H_2, Xe (50:50:1)		
Gas	Helium	Hydrogen	Xenon	Helium	Hydrogen	Xenon
Source Pressure						
PSIA	100	100	100	50	50	1
N/m^2	6.89×10^5	6.89×10^5	6.89×10^5			
Temperature						
500°C (773°K)						
Std cc/sec	$>8.14 \times 10^{-3}$	$>9.02 \times 10^{-6}$	2.03×10^{-7}	8.12×10^{-3}	1.03×10^{-5}	2.03×10^{-7}
Std cc/sec-cm^2	$>2.60 \times 10^{-1}$	$>2.88 \times 10^{-4}$	6.50×10^{-6}	2.60×10^{-1}	3.30×10^{-4}	6.50×10^{-6}
Ratio						
He =			40000 Xe			40,000 Xe
H_2 =	.0011 He		44.31 Xe	.00127 He		50.8 Xe
Xe =	.000025 He			.000025 He		
850°C (1123°K)						
Std cc/sec	6.67×10^{-8}	No flow	2.19×10^{-6}	1.47×10^{-6}	3.69×10^{-5}	3.72×10^{-8}
Std cc/sec-cm^2	2.13×10^{-6}		7.01×10^{-5}	4.70×10^{-5}	1.18×10^{-3}	1.19×10^{-6}
Ratio						
He =			.0304 Xe			39.5 Xe
H_2 =				25.1 He		992 Xe
Xe =	32.91 He			.025 He		
1050°C (1323°K)						
Std cc/sec	9.38×10^{-4}	1.30×10^{-5}	1.51×10^{-4}	9.38×10^{-7}	1.54×10^{-5}	3.12×10^{-7}
Std cc/sec-cm^2	3.0×10^{-2}	4.16×10^{-4}	4.83×10^{-3}	3.0×10^{-5}	4.92×10^{-4}	9.98×10^{-6}
Ratio						
He =			6.21 Xe			30.1 Xe
H_2 =	.0139 He		.0861 Xe	16.4 He		49.3 Xe
Xe =	.161 He			.333 He		

TABLE XII

ROOM TEMPERATURE HELIUM FLOW RATES FOR FILTER 351/133

ZrO_2 0.040 inch OD x 0.089 inch long (1.02×10^{-3} m by 2.26×10^{-3} m)
Cross-Sectional Area = 8.1×10^{-3} cm^2, Density 3.80 gm/cc, L/D = 2.25

Source Pressure		Helium Gas	
PSIA	N/m^2	Std cc/sec	Std cc/sec-cm^2
20	1.38×10^5	2.04×10^{-2}	2.57
40	2.76×10^5	1.20×10^{-1}	1.44×10^1
60	4.13×10^5	2.78×10^{-1}	3.34×10^1
80	5.51×10^5	2.09×10^{-1}	2.51×10^1
100	6.89×10^5	3.14×10^{-1}	3.77×10^1
120	8.26×10^5	4.35×10^{-1}	5.22×10^1
140	9.65×10^5	6.10×10^{-1}	7.32×10^1
160	1.10×10^6	7.13×10^{-1}	8.56×10^1
180	1.24×10^6	9.11×10^{-1}	1.09×10^2
200	1.38×10^6	1.11	1.33×10^2

TABLE XIII

FLOW RATES FOR FILTER 351/333

ZrO_2 0.040 inch O.D. x 0.089 inch long (1.02×10^{-3}m by 2.26×10^{-3}m)

Cross-Sectional Area = 8.1×10^{-3} cm^2, Density 3.80 gm/cc, L/D = 2.25

				Mixed Gases He, H_2, Xe (50:50:1)		
Gas	Helium	Hydrogen	Xenon	Helium	Hydrogen	Xenon
Source Pressure				Not run		
PSIA	100	100				
N/m^2	6.89×10^5	6.89×10^5				
Temperature						
500°C (773°K)						
Std cc/sec	3.34×10^{-1}	3.15×10^{-1}	Not run			
Std cc/sec-cm^2	4.01×10^1	3.78×10^1				
Ratio						
He =						
H_2 =	.943 He					
Xe =						
850°C (1123°K)						
Std cc/sec	3.89×10^{-1}	4.17×10^{-1}	Not run			
Std cc/sec-cm^2	4.67×10^1	5.0×10^1				
Ratio						
He =						
H_2 =	1.07 He					
Xe =						
1050°C (1323°K)						
Std cc/sec	2.02×10^{-1}	2.22×10^{-1}	Not run			
Std cc/sec-cm^2	2.42×10^1	2.66×10^1				
Ratio						
He =						
H_2 =	1.099 He					
Xe =						

APPENDIX A

OPERATION OF RESIDUAL GAS ANALYZER

A residual gas analyzer (RGA) is used to determine the gas leak rate through the filter. The RGA operates in a manner similar to that of a mass spectrometer; i. e., it detects the element in question by deflecting the atom in a magnetic field. The mass of the atom determined the amount of deflection of the atom in the applied field. The RGA "gates" out all atoms except those of the element being sought. The desired atom follows a definite path caused by the magnetic field which is not blocked by gates and is picked up by the detector which, in turn, produces a response level on a strip chart. The RGA can be set to read from 0 to 10, 0-100 to 0 to 1000 (max.) on the strip chart scale. Since the strip chart indicator does not follow a smooth path (see typical scan page A-2), the RGA is adjusted several divisions above the 0 line to compensate for irregularities and to prevent "bottoming" of the recorder pen. This line is called the baseline. When the RGA is adjusted to scan for a given gas (no valves open), the recorder pen will move up several divisions on the scale indicating a given "background" in the system. When the calibrated leak is opened, the recorder pen will rise to a peak response to the leak and then level off. Then, when the leak is valved off, the response will drop back to that of the background reading. Finally, when the unknown leak is opened, a response greater than the calibrated leak is obtained and, when valved off, drops back to background value. In the non-ideal case, the unknown does not drop off when valved because of gas absorption on the system walls. This is strongly apparent when hydrogen is tested.

The calibrated leak is used to calculate the leak rate of the filter by comparing the response of the residual gas analyzer (RGA) to the known and unknown leaks. The calibrated leak has a known leak rate. This known rate is divided by its response minus background plus base on the RGA to obtain the sensitivity of the system. The response of the RGA to the unknown leak is then multiplied by the sensitivity to obtain the leak rate of the unknown leak.

In some instances, the RGA will produce a response that is off the strip chart (in this case >1000). When this occurs, no calculation of flow rate can be made and the only thing that can be said is that the flow is greater than the sensitivity obtained with the calibrated leak, since unknown leak rate = sensitivity x response.

As mentioned earlier, in many cases the background reading is raised considerably after reading the unknown leak due to gas absorption on the system wall. The background is high enough to cause the reading of the next unknown leak to be off the strip chart scale (>1000). In many cases (especially for hydrogen) it is necessary to pump as long as 48 hours to desorb the system so as to reach the same background obtained before testing of the unknown leaks commenced. In each instance that "flooding" of the RGA occurred, the test point was repeated up to four times in an effort to get a determination, but in every case flooding recurred indicating quite high gas concentration in the system.

RGA STRIP CHART SCANS

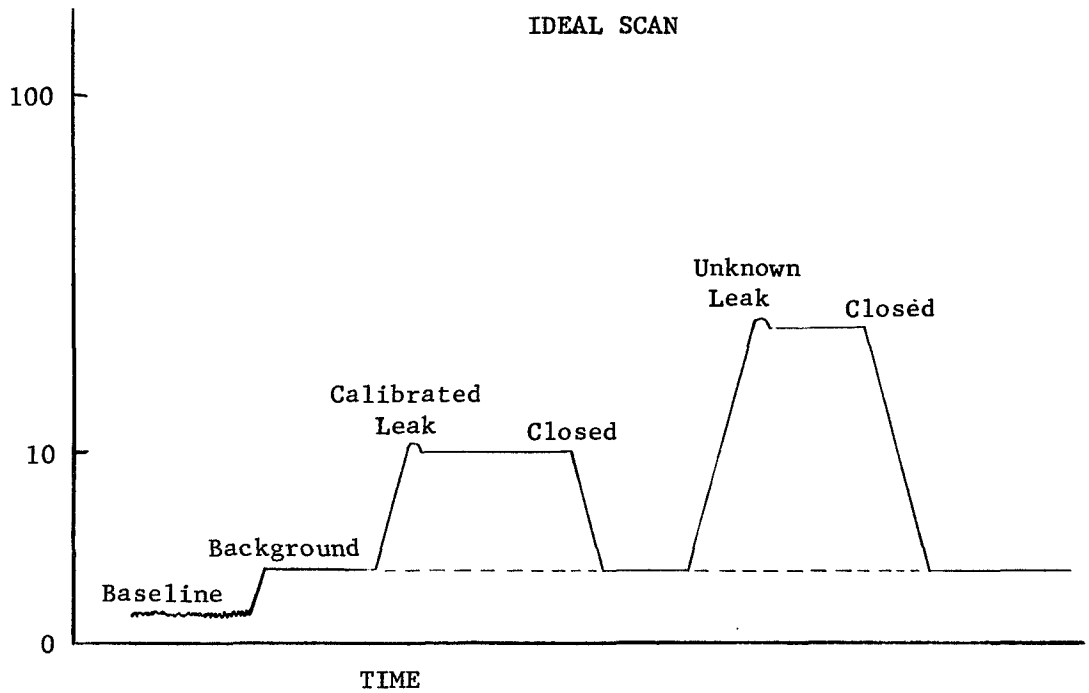

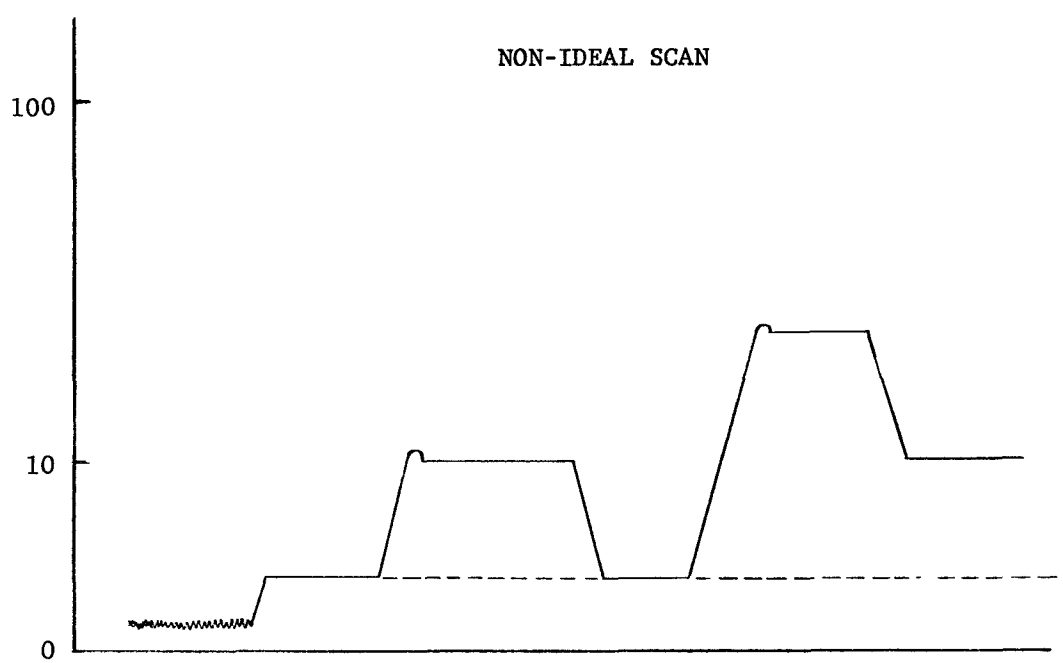

REPORT DISTRIBUTION LIST FOR
CONTRACT NAS3-11839

NASA-Lewis Research Center
21000 Brookpark Road
Cleveland, Ohio 44135
Attention: H. P. Smreker (10) MS 49-2
Patrick M. Finnegan MS 106-1
Richard L. Puthoff MS 106-1
Frank E. Rom MS 106-1
L. V. Humble MS 49-2
B. Lubarsky MS 3-3
John E. Dilley MS 500-309
Library MS 60-3
Report Control Office MS 5-5
Patent Counsel MS 500-311
Tech. Util. Office MS 3-16

NASA Scientific and Technical Information Facility
P. O. Box 33
College Park, Maryland 20740
Attention: NASA Representative

National Aeronautics and Space Administration
Washington, D.C. 20546
Attention: William H. Woodward (RN)
Herbert D. Rochen (RNP)
Charles W. Harper (RD-A)
M. B. Comberiate (RAP)

NASA Ames Research Center
Moffett Field, California 94035
Attention: Mr. Thomas J. Gregory
Library
Hubert M. Drake

NASA Flight Research Center
P. O. Box 273
Edwards, California 93523
Attention: Library

NASA Goddard Space Flight Center
Greenbelt, Maryland 20771
Attention: Library

NASA Langley Research Center
Langley Station
Hampton, Virginia 23365
Attention: Library

NASA Manned Spacecraft Center
Houston, Texas 77058
Attention: Library

NASA Marshall Space Flight Center
Marshall Space Flight Center, Alabama 35812
Attention: Library

Jet Propulsion Laboratory
4800 Oak Grove Drive
Pasadena, California 91103
Attention: Library

U. S. Atomic Energy Commission
Technical Reports Library
Washington,D. D. 20545

U. S. Atomic Energy Commission (3)
Technical Information Service Extension
P. O. Box 62
Oak Ridge, Tennessee 37830

AEC/NASA Space Nuclear Propulsion Office
U. S. Atomic Energy Commission
Washington, D.C. 20545
Attention: Milton Klein

U. S. Atomic Energy Commission
Oak Ridge National Laboratory
P. O. Box 62
Oak Ridge, Tennessee 37830
Attention: Art Fraas

Aeronautics and Space Sciences Committee
Senate Office Building
Washington, D. C., 20510
Attention: James Gehrig

Andrews Air Force Base
Headquarters
Air Force Systems Command
Washington, D. C. 20331
Attention: Major Chiota (SCTSW)
Brig. Gen. R.A. Gilbert (SCT)
Major Gen. G.A. Kent (SCL)
Lt. Gen. C.H. Terhune, Jr. (SCGV)

Arnold Engineering Development Center (AFSC)
Tullahoma, Tennessee 37389
Attention: Mr. Donald W. Male

Kirtland Air Force Base
Albuquerque, New Mexico 87117
Attention: Lt. C. L. Anderson (WLAS-1)
Major Edmund E. Martinez (WLAS) of
Air Force Weapons Lab
Col. James Alderman ;(WLAS-1)

Offutt Air Force Base
Headquarters SAC
Offutt AFB, Nebraska 68113
Attention: Lt. Col. William J. Baugh (DPLB)

Pentagon
Department of Air Force
Washington, D.C. 20330
Attention: Col. R. W. Daniels (JCS)

U. S. Air Force Academy
Colorado Springs, Colorado 80840
Attention: Major Charles M. Bowling
Col. Anthony J. Mione

Wright-Patterson Air Force Base
Dayton, Ohio 45433
Attention: Mr. Fredrik E. Anderson (ASBX)
Mr. John R. Cannon (ASBO)
Mr. Jesse J. Crosby (MAMP)
Mr. Robert Leff (ASBX)
Mr. Robert Barthelemy (APP)
Mr. Stephen M. Nehez (ASBA)
Mr. Lawrence W. Noggle (ASBED)
Mr. Carl L. Oakes, Jr. (ASBS)
Mr. Fred D. Orazio (ASB-2)
Lt. Col. Jay D. Pinson

Battelle Memorial Institute
505 King Avenue
Columbus, Ohio 43201
Attention: Mr. D. Dingee
Mr. S. Paprocki

Beckman Instruments, Inc.
2500 Harbor Boulevard
Fullerton, California 92634
Attention: W. F. Ballhaus

Bell Aerosystems Company
Division of Bell Aerospace Corp.
P. O. Box 1
Buffalo, New York 14240
Attention: Mr. W. H. Dukes

Boeing Company
P. O. Box 3707
Seattle, Washington 98124
Attention: Mr. Jack E. McCormick, MS 2C-8
Mr. Bud Nelson, MS 2C-80
Mr. S. R. Ragar
Mr. George S. Schairer

Cornell Aeronautical Laboratory, Inc.
4455 Genessee Street
Buffalo, New York 14221
Attention: Mr. Larry Bloom

Douglas United Nuclear, Inc.
P. O. Box 490
Richland, Washington 99352
Attention: Mr. R. W. Hallet, Jr.

General Electric Company
Cincinnati, Ohio 45215
Attention: Mr. Peter Kappus

General Dynamics
P. O. Box 748
Fort Worth, Texas 76101
Attention: Mr. H. R. Dvorak
Mr. W. T. Price
Mr. R. N. Widmer (E-14)

General Dynamics/Convair
P. O. Box 1128
5001 Kearney Villa Road
San Diego, California 92112
Attention: Mr. John Wild, Mail Zone 570-00

General Motors Corporation
Allison Division
P.O. Box 24013
Indianapolis, Indiana 46206
Attention: Mr. D. J. Mallon

Georgia Institute of Technology
Atlanta, Georgia 30332
Attention: Prof. Joseph Clement of
Nuclear Engineering Dept.

Isotopes
Nuclear Systems Division
110 West Timonium Road
Timonium, Maryland 21093
Attention: J. W. McGrew
W. R. Seetoo

Lockheed Aircraft Corporation
Lockheed-California Company
2555 N. Hollywood Way
Burbank, California 91502
Attention: Dr. Ronald Smelt, V.P.

Lockheed-Georgia Company
86 South Cobb Drive
Marietta, Georgia 30060
Attention: Mr. F. A. Cleveland
Mr. Roy H. Lange
Mr. M. M. Miller

McDonnell Douglas Corporation
3855 Lakewood Blvd.
Long Beach, California 90801
Attention: Mr. Robert E. Hage

McDonnell Aircraft Co.
Advanced Engineering Department 300
Bldg. 01, Station 24726
St. Louis, Missouri 63166
Attention: Mr. Robert H. Belt

Massachusetts Institute of Technology
77 Massachusetts Avenue
Cambridge, Massachusetts 01239
Attention: Dr. Raymond Bisplinghoff
Prof. Manson Benedict

Pratt & Whitney
400 Main Street
East Hartford, Connecticut 06118
Attention: Library

RAND Corporation
1700 Main Street
Santa Monica, California 90406
Attention: Ben Pinkel

TRW, Inc.
TRW Systems
One Space Park
Redondo Beach, California 90277
Attention: John S. Martinez

Westinghouse Electric Company
Astronuclear Laboratory
P. O. Box 10864
Pittsburgh, Pennsylvania 15236
Attention: Mr. William Budge
Mr. D. G. Ott
Mr. J. E. Werle
Mr. J. W. Niestlie

Aerojet General Corporation
San Roman Plant
P.O. Box 86
San Ramon, California 94583
Attention: Mr. R. H. Chesworth
Dr. H. Jaffe

Atomics International
Division of North American Rockwell
8900 DeSoto Avenue
Canoga Park, California 91304
Attention: Mr. B. B. Shew
Mr. A. B. Martin

Hittman Associates, Inc.
P. O. Box 810
Columbia, Maryland 21043
Attention: Mr. Fred Hittman
Mr. Howard Hagler

Defense Contract Adm. Service Dept.
DCASD Baltimore Bldg. 22
Fort Holebird
Baltimore, Maryland 21219
Attention: J. A. Cooper